

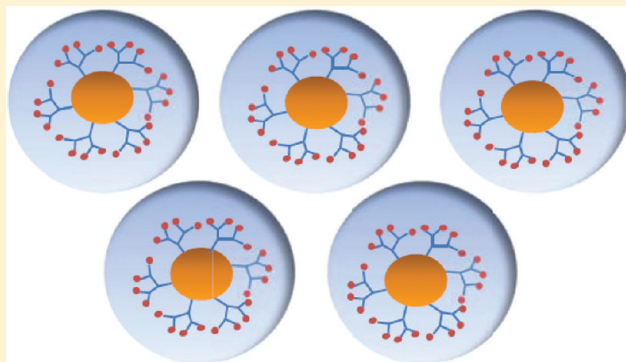
# Hybrid Semiconductor Nanoparticles: $\pi$ -Conjugated Ligands and Nanostructured Films

Yushin Park and Rigoberto C. Advincula\*

Department of Chemistry and Department of Chemical and Biomolecular Engineering, University of Houston, Houston, Texas 77204-5003, United States

**ABSTRACT:** Hybrid inorganic–organic colloidal nanoparticles can be designed to achieve specific and complementary optoelectronic properties different from their sole organic and inorganic counterparts. The efficient coupling between organic and inorganic moieties facilitates optimization of these optoelectronic properties as single particles. Simply dispersing inorganic nanoparticles in an organic (polymer) matrix permits nanocomposite formation, but are usually prone to phase segregation. To achieve more-efficient energy transfer, charge carrier transport, and correspondence between energy levels of the inorganic and organic moieties, direct coupling is necessary. Ligand exchange with highly  $\pi$ -conjugated organic ligands or polymerization of optoelectronically active organic polymer on the surface of the inorganic nanoparticles, results in core–shell-like structures. This increases the surface-area-to-volume ratio contact between organic and inorganic moieties. Because of this advantage, energy transfer mechanism in hybrids can be tuned more efficiently for radiative or nonradiative decay. Recombination of excitons (bound electron–hole pairs) or the isolation of electrons (modulating charge transport) by controlling the conduction band–valence band (highest occupied molecular orbital–lowest unoccupied molecular orbital (HOMO–LUMO)) level becomes more tunable in donor–acceptor materials systems. Such optoelectronic property fine-tuning in a hybrid colloidal system can also be applied toward ultrathin film preparation and two-dimensional patterning (e.g., photovoltaic systems, light-emitting diode materials, sensors, and patterned arrays). A compatible organic shell facilitates greater solubility and dispersion of the inorganic core in a host polymer matrix. The use of a dendronic ligand provides an interesting method for facilitating surface functionalization, nanoparticle solubility, and electrochemical reactivity. By focusing on chalcogenide and semiconductor nanocrystals (NCs) or quantum dots (QDs), it is possible to limit these properties directly to charge carrier transport and energy transfer mechanisms. Each hybrid nanoparticle in essence carries the same properties replicated or dispersed within a film or a pattern. This review focuses on the design, preparation, and properties of such nanomaterial systems.

**KEYWORDS:** nanoparticles, hybrid, conjugated, ligands, films, semiconductor



## 1. INTRODUCTION

A hybrid material has been simplistically defined as a “material composed of an intimate mixture of inorganic components, organic components, or both types of components”.<sup>1</sup> True hybrid organic–inorganic materials are prepared by physical or chemical blending of the organic and inorganic components resulting in desirable or synergistic physicochemical properties not found in their individual components alone. It should also result in a single-phase material that is stable, compared to simple physical mixtures of the two components, which can be prone to phase separation. Controlling the size, composition, and structure of these hybrid materials at the nanoscale and/or molecular to atomic level allows these novel synergistic properties and even new phenomena to be observed with each individual hybrid nanoparticle. Mechanically rigid, electronically active inorganic units combined with flexible, easily functionalizable organic units allow broad processability and applications. Thus, organic–inorganic hybrid materials with controlled functional groups,

chemical composition, and structures should be applicable to a variety of thin-film optoelectronic devices, chemical catalysts, biological sensor, and mechanical (piezoelectric) device applications.

$\pi$ -conjugated or electrically conducting organic molecules and polymers are of high interest for semiconductor and energy conversion devices, because of their ease of processability (often by solution), high energy quantum efficiency, absorption in the visible spectrum, and access from a variety of organic synthetic routes or molecular/macromolecular architectures.<sup>2–12</sup> They can be prepared by chemical oxidative, electrochemical reactions, metathesis, condensation, and metal mediated coupling or cross-coupling reactions.<sup>13–20</sup> In particular, the optical and electronic applications of organic and polymer materials, such as organic light-emitting devices (OLEDs), organic field effect transistors

**Received:** April 27, 2011

**Revised:** July 15, 2011

**Published:** August 02, 2011

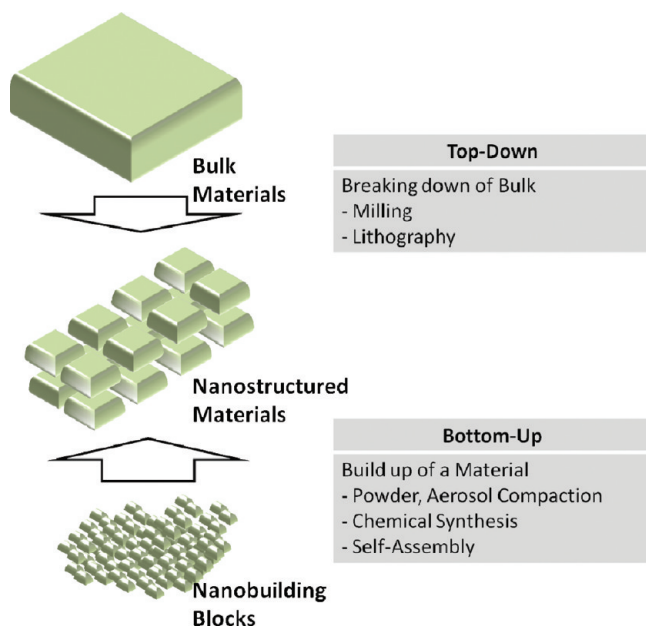


**Figure 1.** Nanostructured materials preparation through the “bottom-up” method and the “top-down” method.

(OFETs), and solar cell devices, are well-reported.<sup>21</sup> On the other hand, solid-state inorganic and metallic materials have a wide range of electronic and magnetic properties, broad atomic selection, and excellent mechanical properties—as utilized in current solid-state device technologies.<sup>22</sup> They have advantages in terms of thermomechanical stability, as well as intrinsically low band-gap (metallic conduction) properties. A disadvantage is their more-demanding processing conditions and limited synthetic scope. Given the complementary properties of organic and inorganic materials, it is indeed a unique challenge to fabricate organic–inorganic hybrid nanomaterials that can have novel and synergistic electro-optical properties and functions of both. The synergic effect of preparing hybrid materials is not only the sum of the properties of organic and inorganic materials blends but also overcoming the limit of each component and achieving enhanced properties as new materials. Through a rational design and optimization, it should be possible to overcome the organic or inorganic limits for a particular processing and device application.

Nanomaterials and fabricated nanostructures are mainly prepared by “top-down”, “bottom-up”, or “hybrid top-down bottom-up” processes. Typically, a “top-down” method of breaking down macrosized bulk materials into micro-sized and nanosized materials has been the traditional route to prepare nanostructured materials, and “bottom-up” method based on designing and building up micro-sized or nanosized modular components is the proper alternative.<sup>23</sup> Because of the limits of the “top-down” approach, such as crystallographic damage and uncontrollable defects, and the limits of the “bottom-up”, such as fabrication problems, even though the “bottom-up” approach allows for a more-homogeneous chemical composition, the hybrid “top-down bottom-up” process (HTBP), which combines both approaches, is used for heterogeneously fabricated nanostructures. In a “top-down” approach, it can be done through laser ablation, selective etching, e-beam lithography, atomic force microscopy (AFM) nanolithography, etc.<sup>24–34</sup> However, it is difficult to achieve homogeneously

structured and monodisperse-sized hybrid materials through this route, much less disperse it uniformly in a host matrix of either organic or inorganic components. Because of enthalpy reasons, aggregation of one component is normally observed and a homogeneous dispersion becomes hard to achieve. To improve the homogeneity of these hybrid materials, a “bottom-up” method is used.<sup>23</sup> The sol–gel colloidal method is an example of a “bottom-up” and “wet synthesis” modular method where controlling the structures and optoelectronic properties of hybrid materials can be designed from exact size, shape, composition, and structures. In this route, the method of preparing hybrid materials can be improved by optimizing colloidal synthesis parameters, allowing greater control in the property of these materials, even at the nanoscale level, compared to the “top-down” method for nanostructuring (see Figure 1).<sup>35</sup>

Semiconductors (mainly chalcogenides), metal oxides, and metallic nanoparticles (NPs) have a large surface-to-volume ratio advantage, which brings about unique physical and chemical properties, compared to their bulk material counterpart, and such properties of colloidal NP materials are applicable in the fields of optics,<sup>36,37</sup> electronics,<sup>38,39</sup> mechanics,<sup>40,41</sup> biological sensors,<sup>42,43</sup> nanomedicine,<sup>24</sup> and storage devices.<sup>44,45</sup> For optical applications, blending with highly  $\pi$ -conjugated and conducting polymers to metals and metal oxides (e.g., polymer/silica nanocomposites) has been well-studied.<sup>46,47</sup> Quantum dots (QDs) can be fabricated within an inorganic glass matrix to have a narrow size distribution, reduced photodarkening, and larger luminescence efficiency.<sup>48–51</sup> Light-emitting applications and electroluminescence enhancement in QD/polymer nanocomposites have been investigated.<sup>52–55</sup> Earlier QD/polymer nanocomposites reported had lower quantum efficiency (<0.1%), which has since increased to 1%–2.5%.<sup>56–60</sup> The electroluminescence properties and external quantum efficiency have been enhanced by adopting the proper QD and polymer pairs. The optical properties of these materials are known to be dependent on their transparency and refractive index modulation.<sup>61–63</sup> For example, the simple blending of SiO<sub>2</sub> NPs and polymers decreases the transparency of nanocomposites, because of the scattering of light triggered by the SiO<sub>2</sub> NPs.<sup>64–67</sup> The transparency of a polymer (e.g., polyimide, polypropylene, poly(methyl methacrylate)) and silica nanocomposites can also be controlled in the matrix by preparing the hybrid materials using the sol–gel method. Organic surfactant-capped noble metallic NPs can be prepared in a similar manner, e.g., nanowires, nanoshells, and nanocages.<sup>68–75</sup> They are very popular and much investigated, giving interesting plasmonic and scattering behavior, which can be identified visible at specific regions of the absorption spectrum.<sup>76–79</sup> The emerging field of plasmonics with interesting theoretical and experimental studies on their size, shape, polarization, localized distance dependence, and field-gradient properties are worth examining carefully.<sup>80–84</sup> However, they will not be the subject of this current review article, in terms of their hybrid properties, because of the limited space and focus on semiconductor materials.

There should be several electrical and energy conversion applications for organic–inorganic hybrid materials. For example, the electrical properties of these hybrid materials can find applications for photodiodes and solar cells. Conventional solar cells have been prepared using inorganic and solid-state materials, such as silicon. These solar cells are said to have suitable efficiencies, but require more-expensive materials and fabrication methods.<sup>85,86</sup> Hybrid materials have been used to substitute the

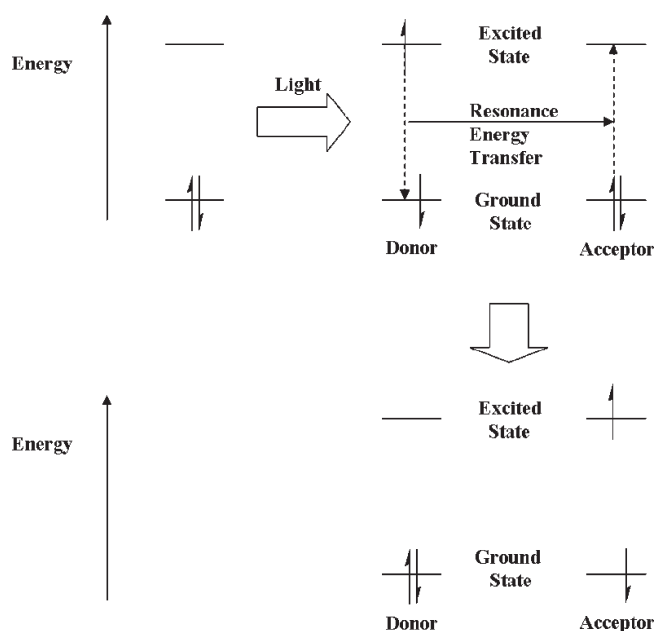


**Figure 2.** Diagram of Förster resonance energy transfer (FRET) from photoexcited donor to acceptor.

inorganic moiety of solar cells, because of their unique electronic properties. In addition, low cost, ease of processing, and thin-film application processing allow hybrid materials to be an alternative for silicon-based solar cells.<sup>87</sup> Blending two materials (donor–acceptor) forms in bulk heterojunction cells can be classified into several types.<sup>88</sup> Blending with highly  $\pi$ -conjugated, optoelectronically active organic polymers enable bulk heterojunction cells, which can be inexpensive, flexible, and processable.<sup>12,89</sup> For example, blending of semiconducting polythiophenes and fullerene derivatives of (6,6)-phenyl-C61-butyric acid methyl ester (PCBM) showed great solar cell efficiency ( $\sim 5\%$ ) and are the most commonly studied.<sup>90–95</sup> Dye-sensitized cell, also known as Grätzel cells, are another type of solar cells or photovoltaic devices.<sup>96</sup> In this case, an electron on the conduction band of the semiconductor, due to the photon, which is absorbed by dye, generates current. Palaniappan and co-workers referred conjugated polymer/QD nanocomposites as another class of bulk heterojunction solar cells.<sup>88</sup> Kamat has classified semiconductor QD utilization in solar cell application in three ways again: polymers/QDs, metal/semiconductor (Schottky junction), and semiconductor sensitized QD solar cells.<sup>97–103</sup> Hybrid organic–inorganic solar cells have since been designed and manufactured by combining conjugated polymers and semiconducting NPs such as  $\text{TiO}_x$ ,<sup>104</sup>  $\text{ZnO}$ ,<sup>105</sup>  $\text{CdSe}$ ,<sup>106–108</sup>  $\text{CdS}$ .<sup>108–110</sup> Alivisatos et al. first reported a photovoltaic device composed of a hybrid blend of inorganic  $\text{CdSe}$  nanorods and organic polythiophene (P3HT), which showed 1.7% solar conversion efficiency.<sup>107</sup>

In general, while the term hybrid nanoparticles can apply to inorganic–organic materials based on noble metals, metals, and metal oxides, this review focuses mostly on semiconductor-based NPs. In particular,  $\text{CdSe}$  nanoparticles are examined, which represent one of the most widely synthesized, studied, and reported materials to date. It should be evident that the properties that will be described and reported with  $\text{CdSe}$  can be extrapolated or covered in depth to other chalcogenide

nanoparticles of the same class and, more specifically, to a particular energy conversion or transfer application (e.g.,  $\text{PbSe}$ ,  $\text{CdS}$ ,  $\text{ZnS}$ , etc.).<sup>111–114</sup>

## 2. ENERGY TRANSFER IN ORGANIC–INORGANIC HYBRID NANOPARTICLES

The energy transfer (ET) theory is a powerful tool for understanding the optical properties of hybrid materials. The ET event tunes the photoluminescence efficiency and changes the emission colors, given that both the donor and acceptor are optically active. Energy transfer can be proved with decreasing or quenching of the emission of donors and increasing emission of acceptor. Because of the energy transfer from donor to acceptor, the excited-state lifetime of the donor is also decreased. It is possible to understand the ET between the organic and inorganic species, as well as the optical properties of hybrid materials by using the concept of Förster resonance energy transfer (FRET). In FRET, the efficiency can be controlled by tuning the overlap function of the emission spectrum of donors and absorption spectrum of acceptors, the distance between the donor and the acceptor, and the optical properties of each moiety.<sup>115</sup>

Sufficient light exposure to donor produces an exciton. Via the resonance between the donor and acceptor, the vibration energy of the exciton is transferred to the neighboring acceptor (normally under 10 nm) in a ground state through FRET (see Figure 2). The basic idea of a “particle in a box” explains the quantum confinement, and the energy of the state is described below:

$$E_n = \frac{h^2 n^2}{8mL^2} \quad (1)$$

where  $h$  is Plank’s constant,  $L$  the length of the box, and  $n$  a natural number. This also shows that the energy (band gap in semiconducting NPs) is decreased as the size of NPs increased. Because of the formation of the conducting band and the valence band, NPs show the absorption and emission bands. The spectral overlap integration can be described as follows:<sup>116,117</sup>

$$J = \int f_D(\lambda) \varepsilon_D(\lambda) \lambda^4 d\lambda \quad (2)$$

Spectral overlap integration is obtained by measuring the donor and acceptor spectral overlap quantitatively over all wavelengths ( $\lambda$ ), depending on the overlapping proportion of  $f_D(\lambda)$ , the normalized emission spectrum of donor, and  $\varepsilon_D(\lambda)$ , the absorption spectrum of the acceptor (extinction coefficient). As FRET occurs, dipole–dipole interaction between the donor and acceptor allows nonradiative emission of the donor, resulting in the emission intensity of the donor decreases and the emission intensity of the acceptor increases simultaneously. Since ET efficiency is dependent on the spectral overlap function of the donor emission and the acceptor absorption, increasing the overlap is a main requirement toward increasing ET efficiency.

The FRET efficiency can be determined experimentally by the ratio of the emission spectra intensity of the donor in the presence of the acceptor to the emission spectra intensity of the donor. The FRET efficiency can be presented as<sup>116,117</sup>

$$E = 1 - \frac{F_{DA}}{F_D} \quad (3)$$



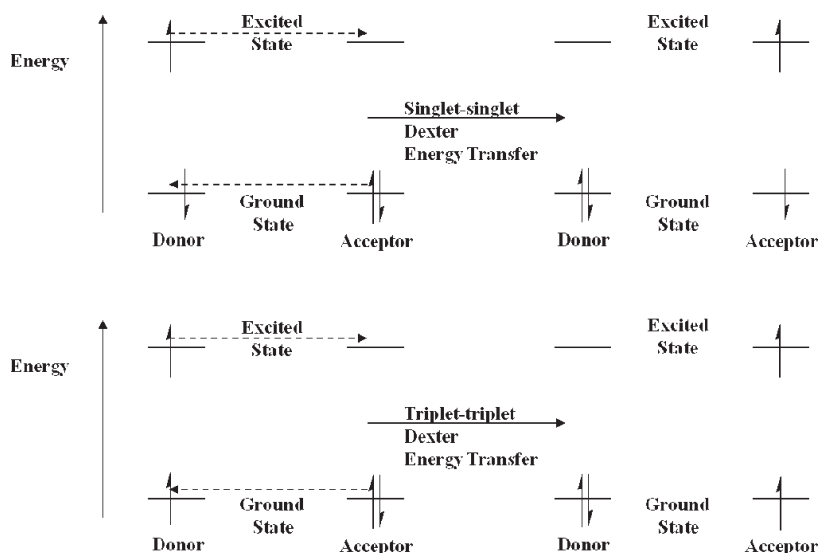


Figure 3. Diagram of the Dexter energy transfer from the photoexcited donor to the acceptor.

where  $F_D$  is the intensity of the emission integration of the donor and  $F_{DA}$  is the intensity of the emission integration of the donor in the presence of the acceptor. In other words, this could be stated as the ratio of decreased emission intensity of the donor in the presence of the acceptor against the original emission of the donor itself. The FRET efficiency can also be presented in terms of fluorescence lifetime, as shown below:<sup>116,117</sup>

$$E = 1 - \frac{\tau_{DA}}{\tau_D} \quad (4)$$

where  $\tau$  is the fluorescence lifetime. It states that the FRET efficiency is the ratio of decreased fluorescence lifetime of the donor in the presence of the acceptor, compared to the original fluorescence lifetime of the donor itself. It is also possible to make a connection that the fluorescence lifetime of the donor is decreased with the FRET process.

The ET efficiency is inversely proportional to the sixth power of the distance between the donor and the acceptor. The Förster radius can be obtained from the calculated FRET efficiency. The Förster radius is related to the FRET efficiency, as shown below:<sup>116,117</sup>

$$E = \frac{nR_0^6}{nR_0^6 + r^6} \quad (5)$$

where  $r$  is the distance between the donor and the acceptor,  $n$  the average number of acceptors related to one donor, and  $R_0$  the Förster distance. From the Fermi golden rule, energy transfer ( $k_{ET}$ ) is related to the interaction elements of the donor ( $F_D$ ) and that of the acceptor ( $F_A$ ) as  $k_{ET} \approx F_D F_A$ .<sup>118</sup> Since it is described as  $F \approx 1/R^3$  with a single dipole,  $F \approx 1/R$  with a 2D dipole, and  $F \approx$  constant with a 3D dipole, it is possible to obtain  $k_{ET} \approx (1/R^3)$  ( $1/R^3 \approx 1/R^6$ ). Energy transfer between core surface of NPs and a dipole could be described as  $k_{ET} \approx (1/R)(1/R^3) \approx 1/R^4$ . Therefore, the higher-order dipole condition distributes more to the energy transfer as the distance decreases. Also, the ET efficiency increases as the distance between energy donors and acceptors is reduced; thus, it is important to keep the donors and the acceptors close to each other. Specifically, this distance should be under 10 nm in order to observe effective FRET. In general, the distance between inorganic and organic species in a hybrid material can be controlled

to meet the FRET distance requirements. Organic ligands (organic) anchored on semiconductor NPs (inorganic) are a good example of such systems. Similarly, the Dexter energy transfer mechanism is also applicable and it is very useful for explaining short-range energy transfer/exchange energy transfer. The Dexter energy transfer mechanism operates by exchanging electrons of donors and acceptors, as shown in Figure 3. It requires not only the spectrum overlap of the donor's emission and acceptor's absorption, but also the wave function overlap for the electron exchange. The rate constant of the Dexter energy transfer can be presented as<sup>119</sup>

$$\kappa = KJ \exp\left(\frac{-2R_{DA}}{L}\right) \quad (6)$$

where  $K$  is an exponential factor,  $J$  the normalized spectral overlap integral, and  $R_{DA}$  the distance between the donor and the acceptor.

**2.1. Preparation of Hybrid Nanoparticles.** As mentioned, the most interesting optical properties of NPs to date are their plasmonic and quantum size effect properties, which are size and geometry (shape) dependent. The size-dependent optical properties of NPs have been studied in Au NPs,<sup>120</sup> conducting Si NPs,<sup>121</sup> Ag NPs,<sup>122</sup> titanium oxides,<sup>123</sup> palladium NPs,<sup>124</sup> lead NPs,<sup>125</sup> nanostructure of copper,<sup>126</sup> and so on. CdSe NPs<sup>127,128</sup> are well-known as size-tunable optical NPs, which are more popularly termed as quantum dots (QDs) or nanocrystals (NCs). They belong to a wider class of chalcogenide semiconductors that have been widely used experimentally.<sup>129–131</sup> Such optical properties of CdSe NPs are applicable for LED devices, biological sensors, and photovoltaic cells. It is also of high interest to investigate the fundamental electro-optical properties of CdSe NPs with new ligand architectures and compositions. It should be evident that the properties that will be described and reported with CdSe can be extrapolated or covered in depth to other NCs of the same class and, more specifically, to a particular application (e.g., PbSe, CdS, ZnSe, etc.).<sup>111–114</sup>

Several synthetic methods have been reported for the preparation of size- and shape-tunable NPs. In general, NPs are <100 nm in size and have large surface-to-volume ratios. There are various types of metallic NPs, which are synthesized either by physical or chemical methods. These methods can further be



classified into gas phase, sol–gel method, and reduction or decomposition method. Many metal NPs have been prepared using a reduction method. Several reducing methods for the preparation of Au NPs were reported.<sup>132,133</sup> Co, Cu, Ag NPs preparations were also reported by the reduction method.<sup>134–138</sup> Metal chalcogenide NCs can be prepared via several methods. Although there are several recipes for nanoparticle synthesis, we will focus on preparing an optoelectronic hybrid nanocrystal system by blending semiconducting nanocrystals with polymers, ligand exchange with photophysically active polymers, or grafting polymers from the nanocrystals in this paper. Generally, nanocrystals are prepared by the nucleation and then growth of ligands by transporting and reacting on the surface of nanocrystals.<sup>139</sup> Murray et al. reported synthesizing monodispersed cadmium chalcogenide NCs via the thermal decomposition method.<sup>125</sup> They mixed dimethyl cadmium and selenium as organometallic precursors in trioctylphosphine (TOP) and trioctylphosphine oxide (TOPO) solutions in high temperature under vacuum.  $\text{Me}_2\text{Cd}$  was mixed with TOP solution in which TOP–Se stock solution by injecting the solution into the heated TOPO up to 300 °C in an argon atmosphere. The solution was removed from heat and cooled suddenly to room temperature to finish further nucleation. Capping the TOP/TOPO reagents slows the steady growth of crystallites above 280 °C. Resulting crystallites have a size distribution of 1.2–11.5 nm. CdSe nanoparticles were centrifuged, adding butanol and methanol to collect size-selective NPs. This colloidal synthesis brought better quantum confinement and size-dependent photoluminescence of the NPs, comparing the old top-down nanoparticle preparation method. Alivisatos et al. reported a CdSe synthetic method that substituted TOP with TBP.<sup>140</sup> A CdSe nanoparticle synthetic method with better size distribution was achieved by Weller et al.<sup>141</sup> The Weller group reported adding hexadecylamine (HDA) as a coordinating component to TOP/TOPO in 2001. They injected a TOPSe and  $\text{Me}_2\text{Cd}$  mixture dissolved in TOP rapidly into the TOPO and HDA mixture heated to 300 °C. In this method, the ratio of TOPO and HDA determines the growth ratio. Increasing the HDA portion decreased the seed size and the growth rate and produced a NP size of  $\sim 5$  nm. Good NP size distribution occurred because a fast focusing process happened in the HDA–TOP/TOPO mixture. Peng et al. replaced  $\text{Me}_2\text{Cd}$  with other Cd organometallic precursors such as CdO,  $\text{Cd}(\text{Ac})_2$ , or  $\text{CdCO}_3$ .<sup>142,143</sup> They could achieve one-pot reaction using CdO. Since they could prepare a stable Cd–HPA complex with  $\text{Me}_2\text{Cd}$  and  $\text{CdCl}_2$ , they could obtain high-quality CdSe NPs in one-pot reaction with CdO. Adding Se solution into the mixture of CdO, TOPO, and HPA, heated to  $\sim 300$  °C, produced high-quality CdSe nanoparticles. In this method, small-sized and monodispersed nanoparticles could be obtained. Geometries of nanoparticles were tunable by controlling the initial monomer concentration. CdO substitution allows CdSe NPs synthesized under milder conditions. Lower injection temperatures of 250–300 °C were required, rather than high temperatures (340–360 °C). Nucleation and growth processes were not dependent on the injection, which allows high reproducibility. Low relativity to the injection for preparing nanoparticle also allows large quantity synthesis with longer injection time. They also published  $\text{Cd}(\text{Ac})_2$ , or  $\text{CdCO}_3$  usage for Cd organometallic sources. In this method, they also applied many possible capping agents and solvents, such as TOPO, fatty acid (FA), dodecylamin (DA), or stearic acid (SA). CdSe NP crystals were obtained by adding Se solution into the mixture of Cd precursors and the

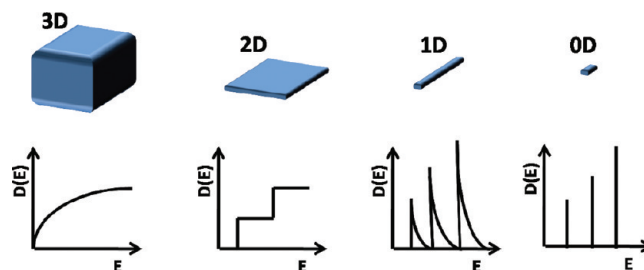


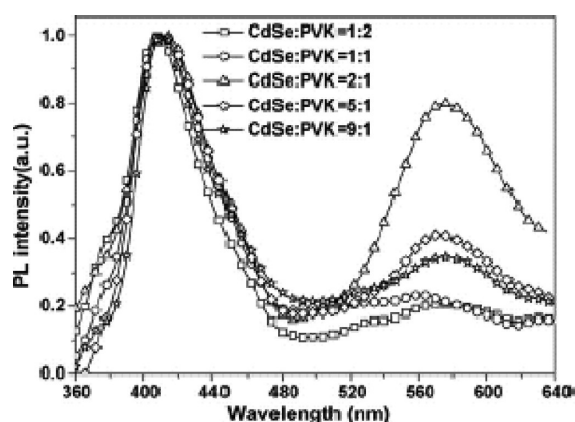
**Figure 4.** Plot of the density of states versus the energy of nanomaterials, depending on the dimensions.

solvents were heated to  $\sim 250$ – $360$  °C. The reaction temperature was  $\sim 200$ – $320$  °C. CdSe NPs were synthesized at temperatures as low as 200 °C with DA, or 130 °C with  $\text{CdCO}_3$  and SA/TOPO. The  $\text{Cd}(\text{Ac})_2$ /TOPO system could achieved better reproducibility than the  $\text{Me}_2\text{Cd}$ /TOPO system, because of the low injection temperature. Such low temperatures applied other reactions using an organometallic source of  $\text{Cd}(\text{Ac})_2 \cdot 2\text{H}_2\text{O}$  were reported.<sup>144</sup> Colvin et al. prepared monodispersed PbSe NCs with PbO and TOP–Se in 1-octadecene and oleic acid.<sup>145</sup> Bawendi et al. prepared monodispersed PbSe NCs using  $\text{Pb}(\text{OAc})_2 \cdot 3\text{H}_2\text{O}$  instead of PbO in phenyl ether and oleic acid<sup>146</sup> and Korgel et al. reported monodispersed  $\text{Cu}_2\text{S}$  nanorods with copper octanoate and dodecanethiol.<sup>147</sup> Besides blending photophysically active organic materials with semiconducting nanocrystals, organic materials can be grafted to (or grafted from) the surface of nanocrystals to achieve optoelectronic properties. Organic monomer or polymer can be grafted to the surface of nanocrystals by ligand exchange. For instance, our group reported phosphonic acid decorated terthiophene dendrons (P3T) or heptathiophene dendrons (P7T) replaced TOPO on the surface of CdSe NCs. Thiophene dendrons and CdSe–TOPO NC solution were stirred for 24 h under a nitrogen atmosphere in chloroform. It was reported that the thiophene dendrons covered the CdSe NCs with 53 and 30 units for P3T and P7T, respectively, with the bulkier P7T replacing the TOPO in smaller numbers.<sup>148</sup> Several methods of “graft from” polymerization on the surface of QDs such as atom transfer radical polymerization (ATRP),<sup>149</sup> reversible addition–fragmentation chain-transfer (RAFT),<sup>150,151</sup> ring-opening polymerization (ROP),<sup>152,153</sup> and oxanionic vinyl polymerization (OAVP)<sup>154</sup> have been reported. The “grafting from” polymerizations with NCs requires fastidious conditions. It is a challenge, because of the instability of the NCs. For example, Emrick et al. grafted poly(*para*-phenylene vinylene) (PPV) from the surface of CdSe NCs through the Heck-type coupling with phenyl bromide and divinylbenzene in the presence of palladium catalyst.<sup>155</sup> Lin and co-workers reported grafting linear vinyl-terminated grafting vinyl-terminated P3HT onto [(4-bromophenyl)methyl] dioctylphosphine oxide (DOPO–Br) functionalized CdSe QDs by Heck-type coupling.<sup>156</sup>

As the size of the NPs decrease, discrete energy states (similar properties to atoms) are observed (see Figure 4), which bring about changes in the optical and electronic properties. Therefore, decreasing the size of a semiconductor to nanoscale makes for novel size- and shape-dependent optoelectronic properties. There have been numerous reports and reviews for preparing the NPs with various shapes and sizes.<sup>157–160</sup> Such dimensions and compositions of NPs have been correlated with their electro-optical properties. Figure 4 shows a plot of the density of states

**Table 1.** Photoluminescence (PL) Intensity Decay Properties of PVK and CdSe:PVK Thin Films<sup>a</sup>

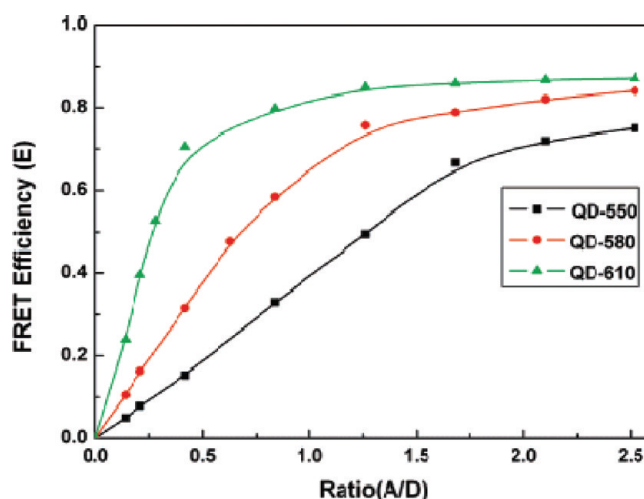
sample	$\tau_1$ (ns) ( $\alpha_1$ (%))	$\tau_2$ (ns) ( $\alpha_2$ (%))	$\tau_3$ (ns) ( $\alpha_3$ (%))	$\tau$ (ns)
PVK	16.9 (41.19%)	4.19 (52.53%)	53.6 (6.28%)	12.5
CdSe:PVK	12.33 (32.54%)	2.41 (64.80%)	76.6 (2.66%)	7.61

<sup>a</sup> Adapted from ref 170, with permission from Elsevier B.V.**Figure 5.** Normalized PL spectra of CdSe:PVK composite films with different mass ratios of CdSe to PVK ( $\lambda_{\text{ex}} = 330$  nm). Adapted from ref 170, with permission from Elsevier B.V.

versus the energy changes, depending on the NPs' dimension. As the dimensions of the nanomaterials increase from dot-shaped zero-dimensional (0D) NPs, to one-dimensional (1D) nanorods and 1D nanocylinders, to two-dimensional (2D) nanodisks, or even three-dimensional (3D) forms, such as tetrapod-shaped nanomaterials, they exhibit different and unique optical properties.<sup>161–167</sup>

In general, the organic ligands on the surface of metallic NPs stabilize the NP system from aggregation and allow the NPs to retain their original size-dependent properties. Aggregation inhibits the hybrid NPs from being homogeneous and achieving size-dependent optical properties. Protecting the NPs with a thin organic ligand (shell) prevents aggregation. It is possible to add electro-optical functionality simultaneous with NP preparation. For example, incorporating highly resonance-stabilized dendrons as capping surfactants leads to effective energy- or charge-transfer phenomena in the NP system.<sup>144,155,168</sup> Furthermore, organic surfactants on the metallic NPs shell enable the system to have greater solubility in organic solvents or water for greater processability as devices. Thus, this review focuses mainly on this energy relationship between the inorganic semiconductor core and the organic ligand functionality.

**2.2. Energy Transfer in Nanoparticle Blends.** During the past several years, the development of OLEDs has been investigated using ET with blends of metallic NPs and organic materials that have electroluminescent properties.<sup>169</sup> Organic–inorganic hybrid materials, which exhibit ET by simply mixing two different light-emitting species, has been commonly employed. For instance, the combination of size-controlled CdSe NCs, and poly(9,9'-dihexylfluorene-2,7-divinylene-*m*-phenylene-vinylene-*stat-p*-phenylenevinylene) (PDHFPV) triggers an ET from the organic PDHFPV to the NCs. In this case, white light

**Figure 6.** FRET efficiency versus ratio of 550-, 580-, 610-nm emitting CdTe quantum dots (QDs) to PTMAEMA-PF-PTMAEMA. Adapted from ref 177, with permission from the American Chemical Society.

was extracted due to the combination of the blue and orange-red lights from the NCs and polymers, respectively.<sup>160</sup> This study also showed the possibility of preparing polymer-based white LED by simple blending of two color species. Similarly, ET was also observed in the blend of poly(*N*-vinylcarbazole) (PVK) and water-soluble CdSe NCs.<sup>170,171</sup> The emission was tunable by controlling the ratio of two species. In this case, the photoluminescence lifetime of PVK was reduced from 12.5 ns to 7.61 ns in solid state by blending PVK with CdSe NCs (see Table 1). This phenomenon shows that ET can occur between the organic PVK and the inorganic CdSe NCs in a simple blend system. The intensity of emission attributed to NC increased until the blend ratio of NC against PVK had a value of 2:1 (see Figure 5). When the ratio went over 2:1, the intensity of the emission started to decrease, because of the quenching caused by the aggregation of the NCs.<sup>172,173</sup> From these observations, it can be clearly seen that the photoluminescence (PL) intensity and the color of the emission can be tuned by mixing NC and organic chromophores precisely.

There are several reports on energy transfer in polymer/nanoparticle blending system, e.g., poly[2-methoxy-5-(2'-ethyl-hexyloxy)phenylene vinylene] (MEH-PPV), poly[(9,9-dihexyl-fluorenyl-2,7-diyl)-alt-co-(9,ethyl-3,6-carbazole)] (PDFC), poly-(2-(trimethylamino)ethyl methacrylate)-polyfluorene-poly(2-(trimethylamino)ethyl methacrylate) (PTMAEMA-PF-PTMAEMA), etc.<sup>172–177</sup> Anni and co-workers reported the ET process in the blending of PDFC and CdSe/ZnS.<sup>176</sup> They observed that PL relaxation gets faster and new relaxation processes appear as the ratio of QDs in the blend increases. Warner and Watt observed similar phenomenon with the MEH-PPV/PbS blend.<sup>175</sup> Similarly, they observed faster PL lifetime decay of MEH-PPV as the concentration of QDs increased in the blend. Wang and Huang also studied FRET between PTMAEMA-PF-PTMAEMA and 550-, 580-, 610-nm emitting CdTe QDs and decreased the PL lifetime of the polymer. They also checked the FRET efficiency change based on the size of CdTe QDs, which is due to the spectral overlap increment as the size of QDs increased, as shown in Figure 6.

### 2.3. Energy Transfer in Nanoparticles: Ligands and Cores.

Since many excellent works have been reported about FRET with

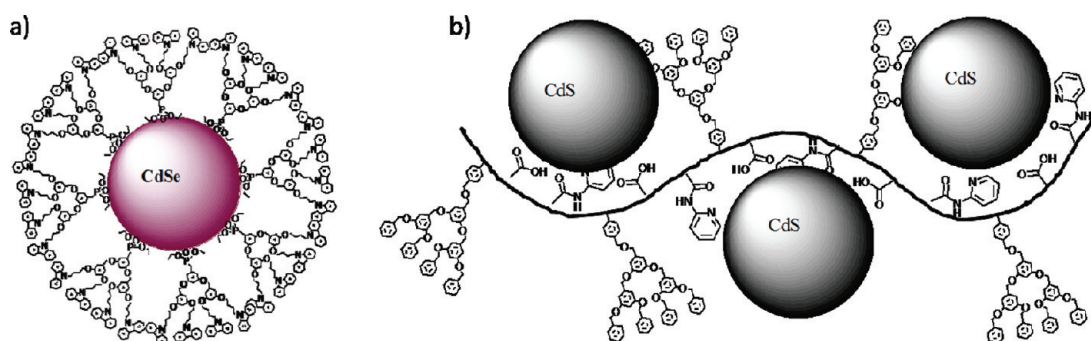


**Figure 7.** Formula of (a) organic–inorganic CdSe hybrid NCs capped with second-generation Fréchet-type polybenzyl ether dendrons (2GPO), and (b) CdS NCs capped with pyridine-functionalized second-generation Fréchet-type dendrons containing dendronized polymers. (The image in panel a has been adapted from ref 168, and the image in panel b has been adapted from ref 187, with permission from Wiley–VCH.)

polymer/QD blends, FRET efficiency is affected by the distance between the donor and the acceptor.<sup>116,117</sup> Fuke and co-workers could get ~100% internal quantum efficiency by reducing the size of the capping ligand on the QDs dots.<sup>178</sup> However, such a blending system has a problem of particle segregation in the polymer and decay of properties over time.<sup>179,180</sup> In case of LEDs, and photovoltaic applications, the surfactants of QDs are stripped during film processing to solve this problem.<sup>181</sup> Therefore, capping QDs with proper organic/polymer ligands would be a method to solve this issue. Emrick et al. reported better energy transfer efficiency and continuous emission from the polymer-capped QDs, compared to the blend system.<sup>182</sup> Electro-optically active organic ligands that cap NC cores not only stabilize NCs from environmental physical aggregation but can also play the role of energy donor or acceptor in an ET process. Organic dendrimer ligands can stabilize semiconductor QD cores from the diffusion of small molecules and ions in the bulk solution, because of the steric crowding cone shape.<sup>37</sup> Furthermore, when organic dendron ligands act as energy donors in the NC system, they can act as an energy antenna. Optically active dendrimers have the site isolation effect, so that they prohibit the self-quenching of the PL of the optically active core by controlling the intermolecular interaction.<sup>183–186</sup> As mentioned previously, optically active organic ligands capped NCs can be prepared by direct synthesis using sol–gel colloidal methods. Direct synthesis means that the ligand is first synthesized and used to cap the growth of the NC without doing a ligand exchange reaction to get the desired shell. Through this synthesis method, it is possible to maintain most of the original optical properties of the NC. However, it is a challenging task to optimize the synthetic conditions, such as temperature, stoichiometry of reactants, reaction rates, and so on. Similarly, optically active ligands based on dendrons, such as carbazole-bearing second-generation Fréchet-type dendrons, covering the NCs, have been directly synthesized.<sup>168</sup> In one approach, phosphonate-functionalized second-generation polybenzyl ether dendrons (2GPO) were used as a capping reagent for CdSe NCs (see Figure 7a). The carbazole-bearing dendron-capped CdSe NCs had ET properties between the capping agent of 2GPO and the CdSe NC core. The absorption intensity of the 2GPO-capped NC solution increased linearly with the concentration of the NC solution.

However, the PL of carbazole subunits decreased and that of the NC cores increased as the concentration of NC solution increased. This is due to the ET from the peripheral carbazole

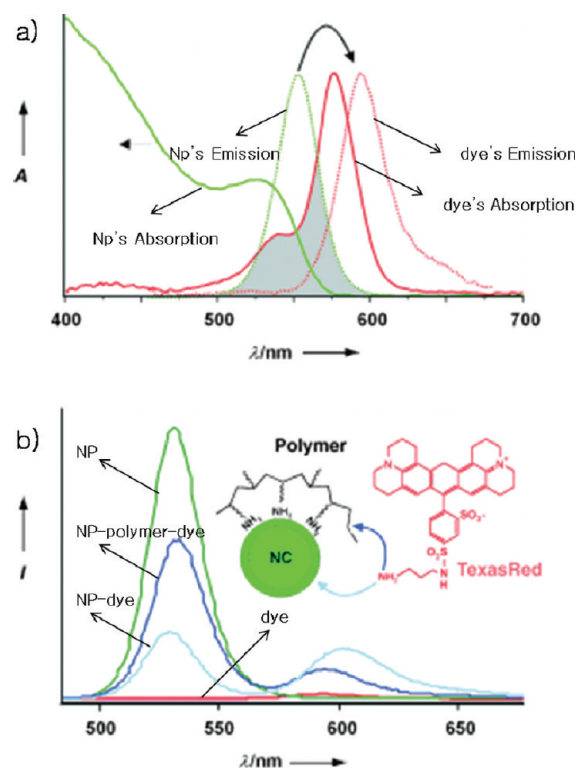


**Figure 8.** (a) Absorption and emission spectra of the NCs and the dye (TexasRed (TR)) in solution. (b) Fluorescence spectra of the NCs, dye, NC–polymer–dye, and NC–dye, respectively, upon excitation at  $\lambda = 488$  nm. (Panels a and b have been adapted from ref 188, with permission from Wiley–VCH.)

subunits to the NC cores, and the quantum yield was 14.5%. The dendronized polymer was used as a capping reagent to form the dot-shaped NCs into one-dimensional tube-shaped features (see Figure 7b).<sup>187</sup> CdSe NCs capped with the pyridine and the second-generation Fréchet-type dendrons-bearing polymer formed inorganic/organic necklace hybrids have been reported.<sup>148</sup> This is due to the retention of the polymer backbone instead of the formation of structuring individual particles.

Ligand exchange (LE) is a facile alternative method for capping NC surfaces with new organic ligands. Substitution of the terminal functional group of the organic ligands is a



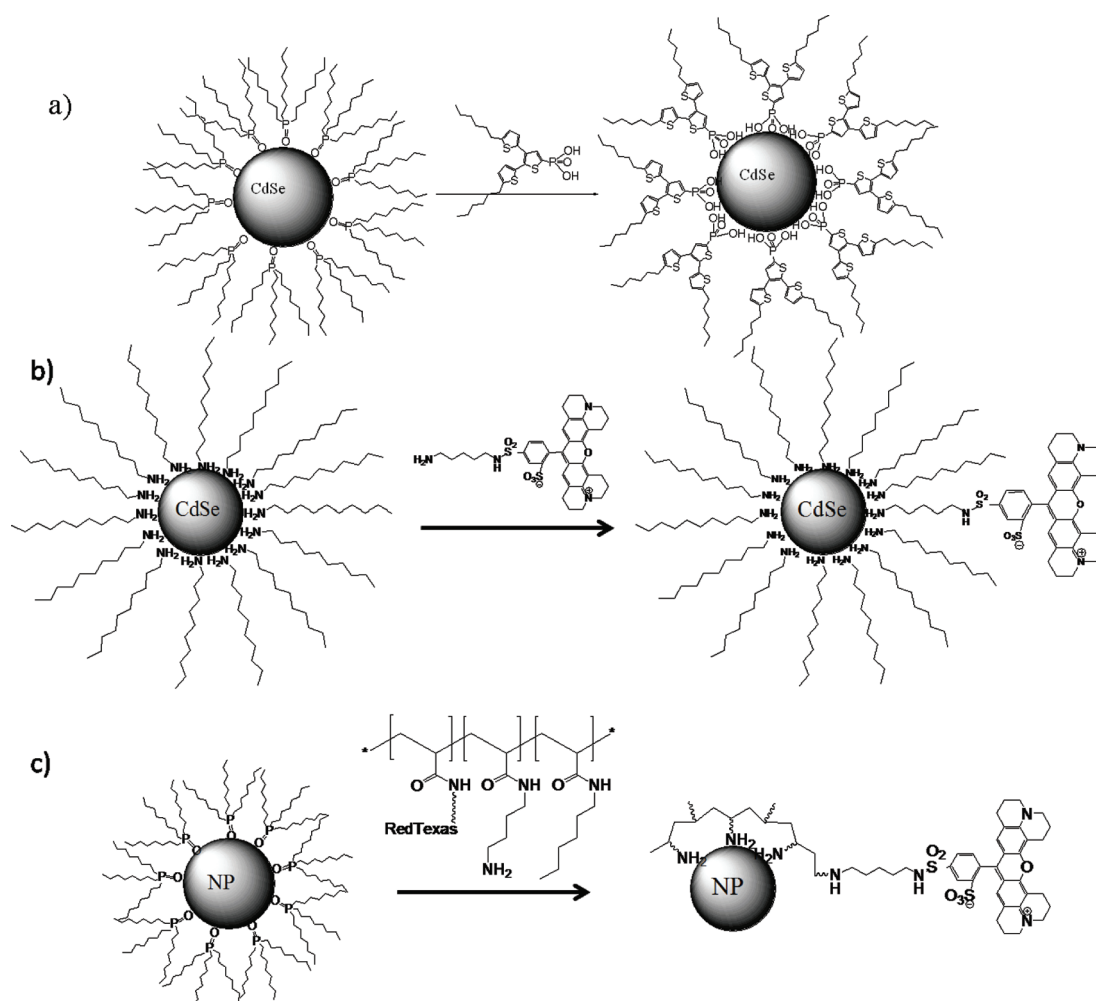


**Figure 9.** ET in ligand exchanged NCs. (a) P3T replaced TOPO, (b) amine-functionalized TR replaced alkyl amine, and (c) TR-bearing polymer replaced TOPO on the surface of NCs. (Panel a has been adapted from (a) ref 148, with permission from the American Chemical Society; panels b and c have been adapted from refs 189 and 188, respectively, with permission from Wiley–VCH.)

prerequisite for LE. It requires functionalizing the terminus of the organic ligands to allow stronger interaction with the NC cores such as phosphonic acids, thiols, or amines, etc. The LE method allows many types of dendrons (including bulky dendrons) for capping NC cores with proper functional groups. This is based on a “gradient” approach, with respect to ligand–metal interaction, where a stronger interaction replaces a ligand with a weaker interaction. The weaker ligand was originally used to cap the growth kinetics of the NC. For instance, optically active dendrons, such as thiophene dendrons, can replace TOPO and cap the NC cores of CdSe–TOPO NC through the LE method. ET also worked by exchanging TOPO with amine-functionalized TexasRed (TR) or amine-functionalized TR-bearing polymers on CdSe/ZnS core–shell NCs (see Figure 8b).<sup>188</sup>

Amine and alkyl group-decorated polymer chains ( $n \approx 200$ ), which contains approximately one molecule unit of TR, replacing the TOPO from the CdSe/ZnS core–shell NCs has been reported. This polymer was designed to have  $\sim 100$  amine subunits, which produces a stronger interaction with the NC. The polymer replaced TOPO by repeating the process of dissolution and precipitation in pyridine. TR-capped NCs or TR-bearing polymer-capped NCs produced stronger PL from TR and decreased PL from the NCs, because of the efficient ET

mechanism from NCs to dyes (see Figure 8). The TR-bearing polymer-capped NC showed a stronger PL intensity than that of TR alone but gave weaker fluorescence intensity than that of the NCs alone. The TR-bearing polymer, which was functionalized with several units of amine for anchoring, was more stable than the amine-functionalized TR on the surface of the NCs. This stability difference also explains the difference in ET efficiency between those two hybrid materials.

One of the disadvantages of the LE method is that it is impossible to replace all of the original capping reagents with the intended ligands completely in one step. However, it has been reported that the favored ligands could be replaced completely by a two-step LE: (1) replacing the original ligands with pyridine and then (2) replacing pyridine with the favored ligands.<sup>148</sup> It is possible to tune the optical properties of the NC, even with incomplete LE, from an optoelectronic point of view. It has been reported that substituting one molecule out of the original capping ligand was enough to alter the PL of the NCs (see Figure 9).<sup>189</sup> The emission of the NC was quenched by LE. It was found that the LE with one molecule of the amine-functionalized TR was enough to completely quench the emission of the NCs (see Figure 10). LE was performed with octylamine-capped CdSe

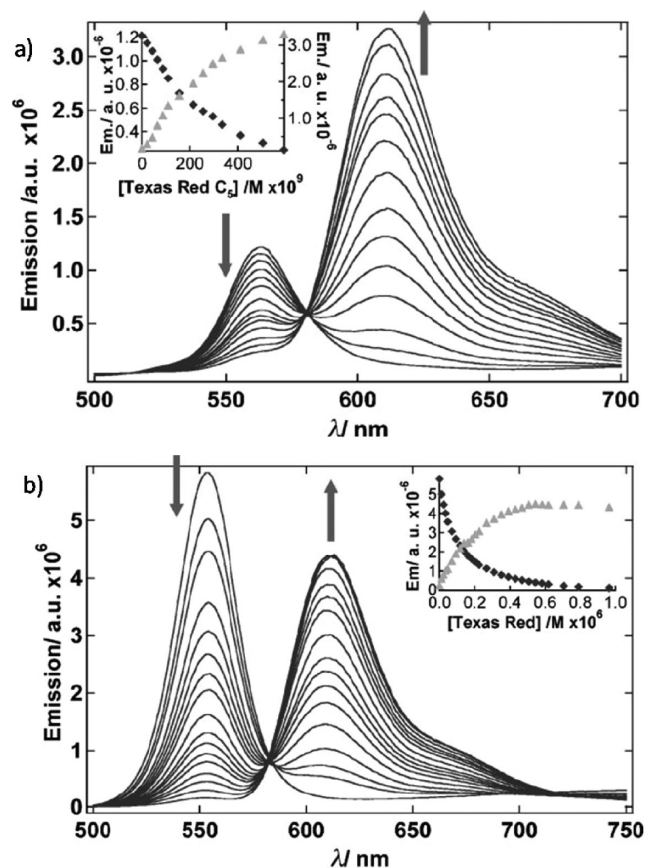


**Figure 10.** (a) Energy transfer (ET) from the CdSe NC to the ligated dye TR (610 nm) with increasing dye concentration (inset shows the fluorescence at 563 nm (diamonds) and 610 nm (triangles), as a function of TexasRed C5 concentration). (b) ET from the CdSe NC to the ligated dye TR. (Panels a and b have been adapted from ref 189, with permission from Wiley–VCH.)

NCs or nanorods, and amine-functionalized TR or Lissamine Phodamine B Ethylenediamine (LRhBen).

This experiment showed that the NC's emission intensity decreased and the dye's emission intensity increased, because of the effective ET. They compared the predicted values and the experimental data to calculate how many dye molecules were needed to activate or quench the PL of the donor and the acceptor via the LE method. They calculated that one molecule of the dye compound was indeed enough to make the ET occur from the NC to the dye. They also found that replacing 1.85 dye molecules on the surface of the NC increased the emission band area by a factor of 3 more than the emission band area of the NCs alone (i.e., those not capped with dyes). They also reported that 20% of the dyes were adsorbed onto the NCs through LE if the dyes competed with the original ligands (octylamine) in the presence of excess ligands. The quantum yield of the modified NC by ligand exchange with dyes is much greater than that of the NCs without LE.

The ligands extending from the surface of the NCs through a "grafting from" technique is another alternative method of capping NC core with favored organic ligands. Linear polymers, even though they are not optically active, can be grown via the "graft from" method, which involves grafting the aniline tetramer on the surface of NCs by forming an imine (see Figure 11a).<sup>190</sup>

There are a few reports for coupling reactions of highly extended conjugated system using catalysts for ET. Emrick et al. reported CdSe NC-poly(*para*-phenylene vinylene) (PPV) (CdSe NC-PPV) synthesis with phenyl bromide and divinylbenzene (see Figure 11b).<sup>155</sup> This coupling reaction allows NCs to be dispersed more uniformly, since the blend of NCs and PPV exhibited aggregation. Furthermore, CdSe NC-PPV prepared by coupling reactions showed a strong emission of NC (570 nm) and a weak emission of PPV (440 nm) (see Figure 11d), compared to the blends of CdSe NCs and PPV (see Figure 11c).

Dominant PPV emission peaks appeared in the blends of the NC. However, PPV emission completely disappeared in the case of an NC-PPV. In the solid state, the strong emission of the NC appeared with a relatively small (2–5 wt %) concentration unlike the large amount required of direct mixing of NCs in blends. This was because the contact area was not reduced in the case of the CdSe NC-PPV and polymers. Also, aggregation that can form in the blend was avoided, which can result in the self-quenching of NC's emission. In another case, oligophenylene vinylene (OPV) was extended on the surface of the NCs. NC-OPV was synthesized via the "graft from" method and also showed higher intensity of NC emission than that of the NC-OPV blend.<sup>191</sup>

**2.4. Energy Transfer between Nanoparticles.** Because of the size-dependent optical properties of the NCs, ET is also possible between different-sized NCs. It has been reported that ET was observed from small NCs to large NCs by controlling the size and arrangement between those NCs.<sup>192</sup> When the size of the NC increased, the band gap between the highest occupied nanocrystal orbital (HONCO) and the lowest unoccupied nanocrystal orbital (LUNCO) decreased, so that the ET is more probable from small NCs to large NCs.

CdTe NCs in four different sizes (in the range of 1.7–3.5 nm) have been prepared, and the absorption and emission spectra have been examined.<sup>192</sup> As a reference, the PL of the film consisting of several layers of 3.5-nm CdTe NCs was comparable to the PL of the film with layers of four different-sized CdTe NCs. The PL intensity of the film that had cascade layers with different-sized CdTe NCs was much larger than that of the sequentially layered (3.5 nm) CdTe NCs film (see Figure 12b). They explained this phenomenon such that the trapped excitons were transferred to the larger-sized NCs. Different-sized NC films, compared with the one-sized NC reference that decayed 98% of the excitons nonradiatively, resulted in the higher PL intensity of the NCs.

ET between NPs, which is designed to interact with biomaterials, is usually applicable in biosensors. In one example, a glucose-detecting biosensor was designed with ET mechanism elimination by breaking the interaction between two different NPs via glucose replacement (see Figure 12a).<sup>193</sup> Concanavalin A (ConA) conjugated CdTe NCs and  $\beta$ -cyclodextrins ( $\beta$ -CDs)-functionalized Au NPs transfer energy from CdTe NCs to the Au NPs through FRET due to the interaction between ConA and  $\beta$ -CDs. ConA is also able to interact with glucose above pH 7. The introduction of glucose to the CdTe NC-ConA- $\beta$ -CDs-Au NPs to form CdTe NC-ConA-glucose degenerated the ET. Consequently, the emission of the CdTe NCs was increased by breaking the CdTe NC-Au NP, destroying the FRET mechanism (see Figure 12c). Increasing the amounts of glucose increased the emission of the CdTe NCs, showing a direct correlation between CdTe NC emission and glucose concentration.

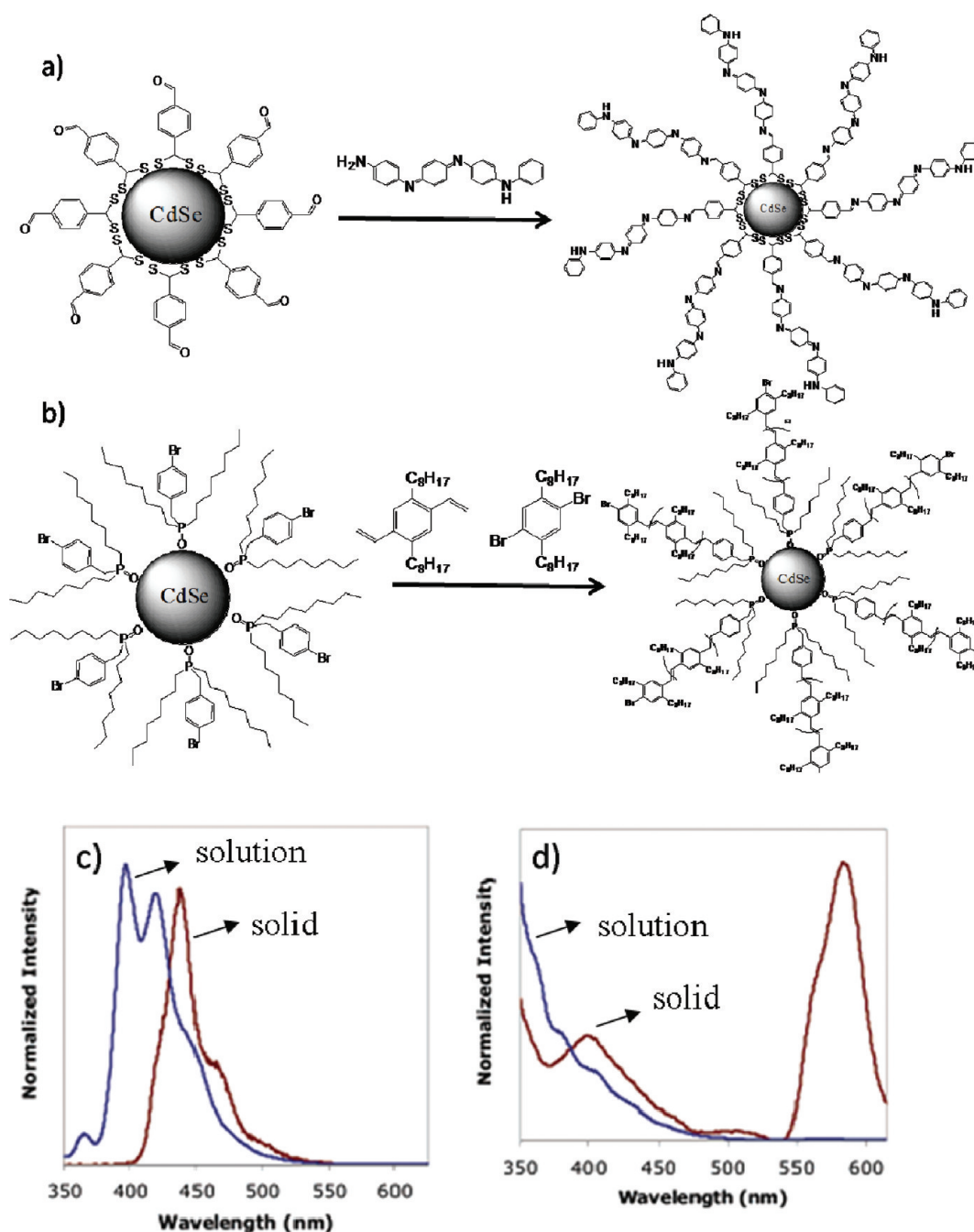


**Figure 11.** ET in “graft from” extended NCs ((a) grafting aniline tetramer and (b) grafting phenyl bromide and divinylbenzene on the surface of NCs). Photoluminescence spectra of (c) bromophenyl-functionalized CdSe NCs blended with PPV and (d) PPV-functionalized CdSe NCs. (Panel a has been adapted from ref 190, with permission from the Royal Society of Chemistry; panels b–d have been adapted from ref 155, with permission from the American Chemical Society.)

**2.5. Hybrid Nanoparticle Films.** Film preparation is an important step for the application of hybrid materials and their unique optical properties for devices. In the solid state, the interaction between each component is more restricted than in solution. Distance between organic and inorganic species is also important, because the components are not as mobile as in a solution state. In case of photovoltaic cells, better dispersion of the QDs in an optoelectronic active polymer matrix allows better charge separation.<sup>194</sup> Also, the orientation of ultrathin and flat films is important for device geometries and performance.<sup>195</sup>

Therefore, homogeneous dispersion methods have been used to prepare hybrid materials with well-defined structures in the nanoscale.<sup>68,97,196,197</sup> However, it is also important to connect nanomaterials to nanomaterials for the conduction path of the device.<sup>198–200</sup>

The most general, if not simplest, approach to prepare hybrid thin-film materials is by simply mixing the two components with different composition ratios and spin-casting or solvent-casting the films. The problem with these materials is the lack of compatibilization between the inorganic NCs and the conjugated



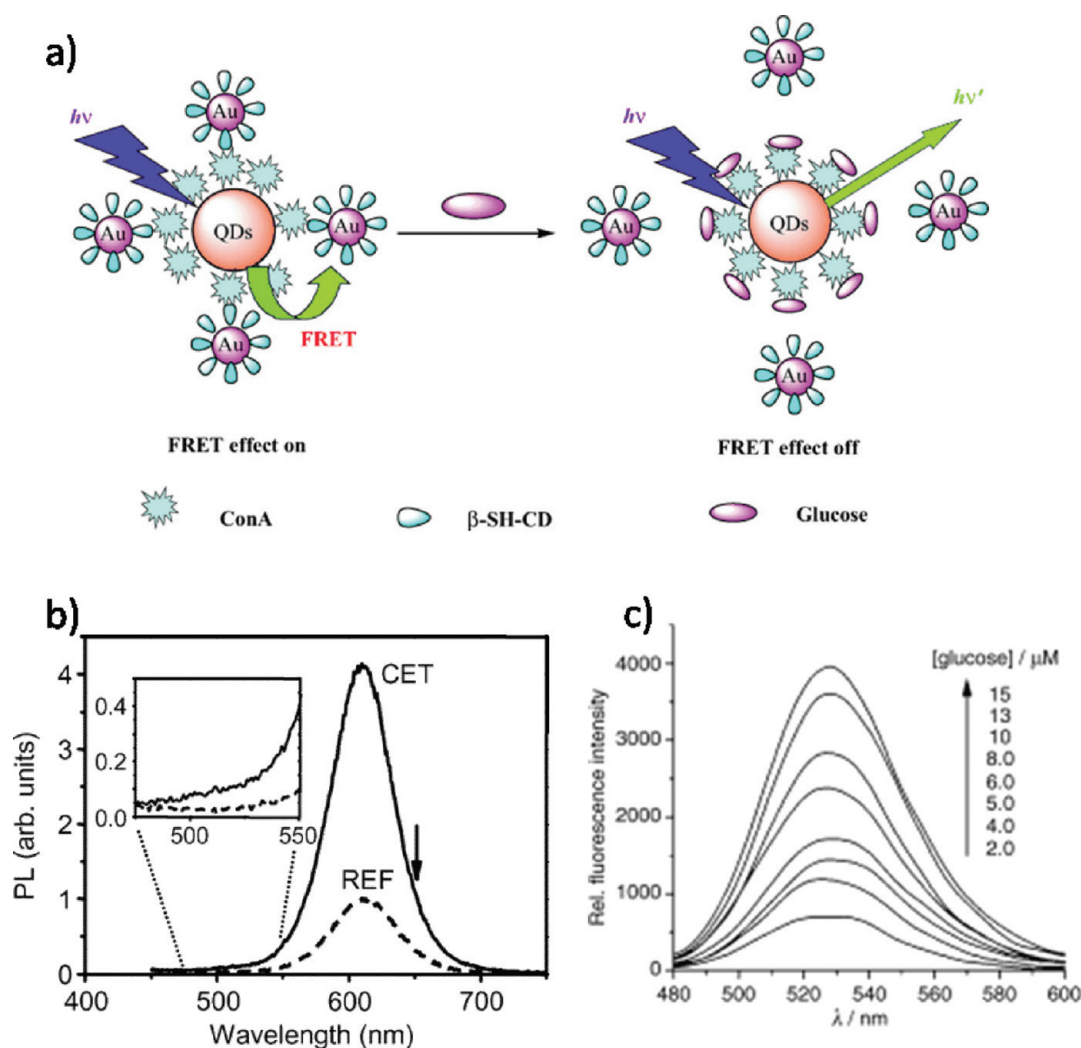


**Figure 12.** ET between NCs: (a) glucose separates two NCs and blocks ET, (b) the PL intensity of different-sized CdTe NCs was much bigger, and (c) the PL intensity of NCs increased with increasing glucose concentration by blocking the ET between two NCs. (Panels a and c have been adapted from ref 193, with permission from Wiley–VCH; panel b has been adapted from ref 192, with permission from the American Chemical Society.)

polymer matrix resulting in phase separation or a loss of ET efficiency over time.<sup>68,97,196,197</sup> Well-designed and well-structured films in the nanoscale are possible with specific film preparation techniques, such as layer-by-layer (LBL),<sup>201,202</sup> Langmuir–Blodgett (LB),<sup>203,204</sup> and electrodeposition.<sup>37</sup> Because of the nature of organic–inorganic hybrid materials, it is possible to prepare electrically charged NCs. Interactions between charged ligand-capped NCs, metal ions, and charged organic materials allow them to pack and interact better, improving their optoelectronic properties. Nurmikko et al. reported ET in the LBL film, which consists of J-aggregated dyes and CdSe–ZnS core–shell NCs (see Figure 13a).<sup>202</sup> They prepared NCs capped with 11-mercaptopundecanoic acid (MUA) and J aggregate dye of 5,6-dichloro-2-[3-[5,6-dichloro-1-ethyl-3-(3-sulphopropyl)-2(3H)-benzimidazolium]-1-propenyl]-1-ethyl-3-(3-sulpho-propyl) benzimidazolium hydroxide (TDBC) as the negatively charged sources for LBL. These optically active materials were electrostatically glued with poly(diallyldimethylammonium chloride) (PDDA), which is positively charged. The thickness of TDBC/PDDA bilayer was  $\sim 3.3$  nm and the NC and dye layers were close enough to allow

for ET. In this experiment, two different NCs were applied to tune the ET flow from NCs to dyes or from dyes to NCs.

In these LBL films, the materials were designed to have ET from NC to the dye. The emission of the NC was quenched by  $\sim 98\%$ , and the emission of the dye appeared to be dominant (see Figure 13c). In contrast, ET from the dye to the NCs led to a strong emission from the NCs. ET in the LBL film involves not only in the NC and the polymer dye combination, but also the different-sized NCs, as previously mentioned.<sup>205</sup> Klimov et al. prepared two different-sized (1.3 and 2.05 nm) CdSe/ZnS core/shell NCs and assembled NCs in monolayer-by-monolayer structure for light-harvesting NC films.<sup>205</sup> Dithiol-functionalized molecules were used to link two different-sized NCs covalently and the distance between these two NCs was  $\sim 6.2$  nm. The PL of the smaller NCs in the LBL film was depleted almost completely within 5 ns, yet that of the large NCs decreased insignificantly (see Figure 13d). This indicates that efficient ET from small NCs to large NCs in LBL films is possible. As mentioned previously, LBL-assembled NCs films also achieve ET among several different-sized NCs (see Figure 13b).<sup>192</sup> Thioglycolic acid-capped NCs were negatively

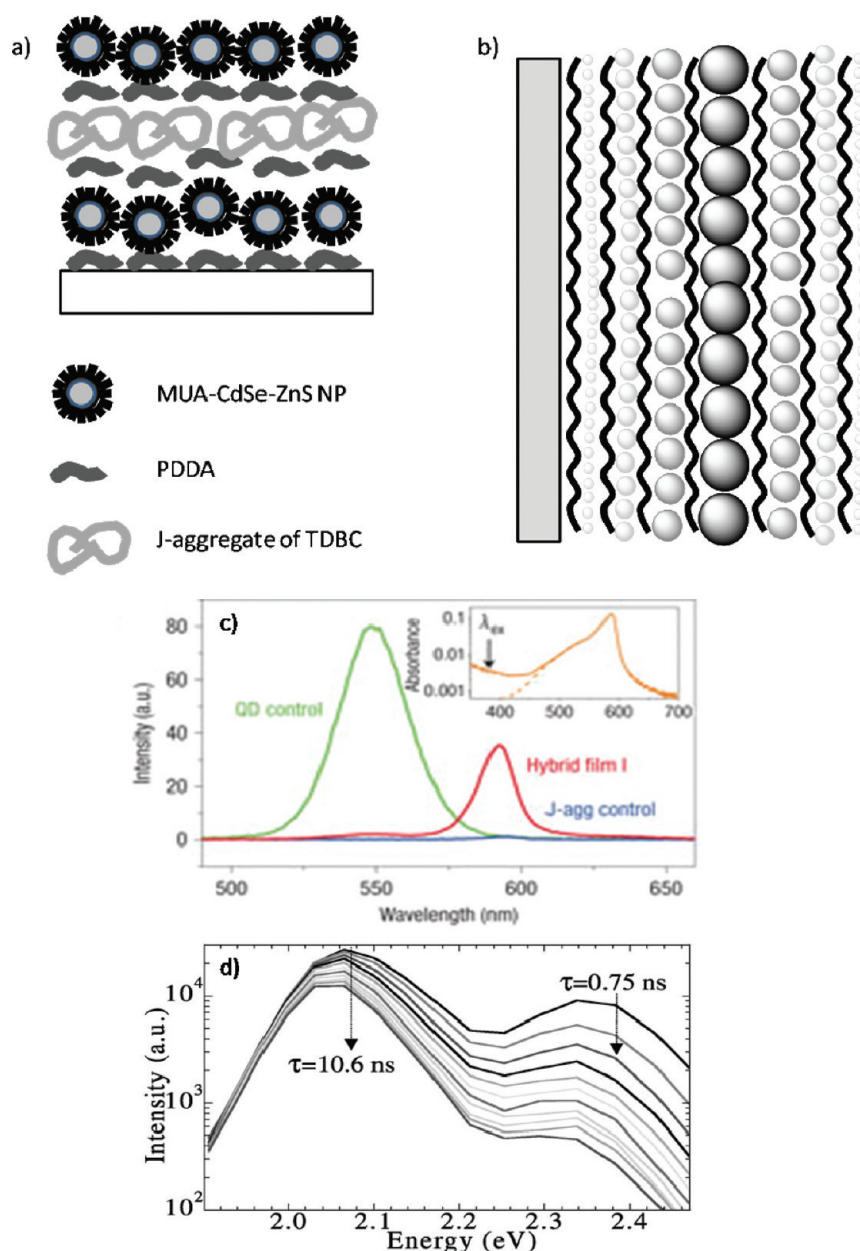


**Figure 13.** ET in a layer-by-layer (LBL) hybrid NC film: (a) LBL films of NCs and polymers, (b) LBL films of different-sized NCs, (c) NC's emission was quenched  $\sim 98\%$  in the NCs and polymer LBL film, and (d) PL of smaller NCs in the monolayer-by-monolayer film depleted almost completely in 5 ns. (Panels a and c have been adapted from ref 202, with permission from Nature Publishing Group; panel b has been adapted from ref 192, with permission from the American Chemical Society; and panel d has been adapted from ref 205, with permission from the American Physical Society.)

charged under slightly basic conditions. Positively charged PDDA and negatively charged NCs were held together as electrostatic LBL films. The largest-sized CdTe NCs were layered in the middle of two layers of the smaller-sized CdTe NCs. ET from both ends of the LBL films into the middle NC layer was observed.

The Langmuir–Blodgett (LB) film technique is another useful technique used to prepare hybrid thin films for optoelectronic applications. It was reported that the thin-film preparation of NCs to form quantum well structures by the LB technique achieved noncontact, nonradiative ET with 50% ET efficiency.<sup>206</sup> Monolayered CdSe/ZnS core/shell NC films were prepared by the LB technique onto the InGaN quantum well layers, deposited

on the GaN bottom layer by metal–organic chemical-vapor deposition. The ET occurs via the FRET mechanism, relying on Coulombic interaction rather than donor–acceptor overlap. Achermann et al. examined the time decay of PL for the quantum wells with or without NCs for ET rate studies.<sup>207</sup> The PL of the quantum well decayed faster in the presence of the NCs. This indicated that a FRET occurred from the quantum well structure to the NCs. The PL of the NCs also increased when the NCs were coated. It is convenient to detect target materials by PL quenching of monolayered NCs by interaction with another NCs.

Ying et al. used the LB technique to prepare a ZnS–CdSe core–shell NC thin film for biosensing.<sup>208</sup> They prepared

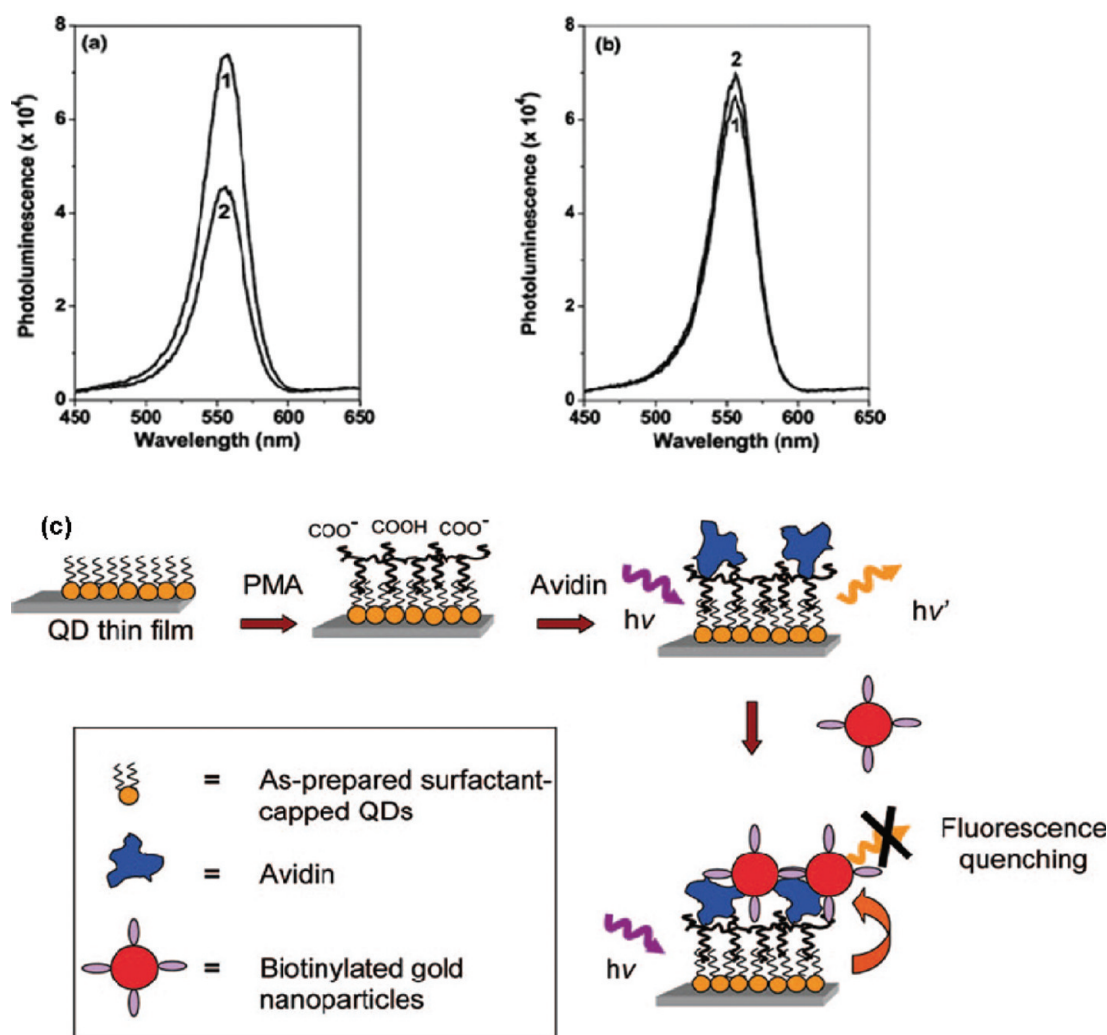


**Figure 14.** Fluorescence spectra of TOPO-ODA–ZnS–CdSe films that are modified with (a) PMA–avidin and (b) PMA–streptavidin, (1) before and (2) after introducing Au NCs. (c) Synthesis scheme of surface-modified NC thin films. (All panels have been adapted from ref 208, with permission from the American Chemical Society.)

single- or multilayered films of TOPO-octadecylamine (TOPO-ODA) and TOPO-tetradecylphosphonic acid (TOPO-TDPA)-capped NCs via the LB technique. They also modified the hydrophobic surface of NCs to have hydrophilic properties by applying self-assembled poly(maleic anhydride-alt-1-tetradecene) (PMA) on the NC layers to interact with proteins or target materials. The carboxylic acid functional group of PMA anchors to avidin, which is attracted to biotinylated Au NPs on the PMA-NC thin film (see Figure 14c). This interaction between Avidin-PMA–ZnS–CdSe NC thin films and biotinylated Au NPs allows for ET from ZnS–CdSe-NCs to the Au NPs. In the presence of avidin, Au NP adsorbs onto the ZnS–CdSe NCs thin film, reducing the PL of ZnS–CdSe NCs by FRET quenching (see Figure 14). However, the presence of streptavidin on the ZnS–CdSe NCs thin film with Au NPs did not decrease the PL intensity of ZnS–CdSe NCs.

### 3. CHARGE TRANSFER IN ORGANIC–INORGANIC HYBRIDS

Gregg classified solar cells into two groups: conventional solar cells and excitonic solar cells.<sup>206</sup> Excitonic solar cells can be classified again as organic photovoltaic cells, dye-sensitized

solar cells (Grätzel cells), and cells made from small molecules, polymers, and QDs that belong to the excitonic solar cells class.<sup>68,209–211</sup> When free electron–hole pairs are produced in the most conventional inorganic solar cells, bound electron–hole pairs (excitons) are produced when excitonic solar cells absorb light.<sup>209,212</sup> The external quantum efficiency ( $\eta_{EQE}$ ), the ratio of the number of electrons flowing in the cell to the number of injected photons, of the excitonic solar cells can be presented as<sup>68,213</sup>

$$\eta_{EQE} = \eta_A \eta_{ED} \eta_{CC} \quad (7)$$

where  $\eta_A$  is the absorption efficiency,  $\eta_{ED}$  the exciton dissociation efficiency, and  $\eta_{CC}$  the carrier collection efficiency.<sup>68,213</sup> Since the external quantum efficiency is an essential factor indicating the charge transport properties of the excitonic solar cell, it is important to consider the three conditions for the device operation.<sup>214</sup> Photon incidence generates excitons and photo-induced excitons, bound electrons and holes, which move to the interface of the donor and acceptor. The excitons must be dissociated into separated electrons and holes to produce photocurrent. In an ET process, photogenerated electrons and



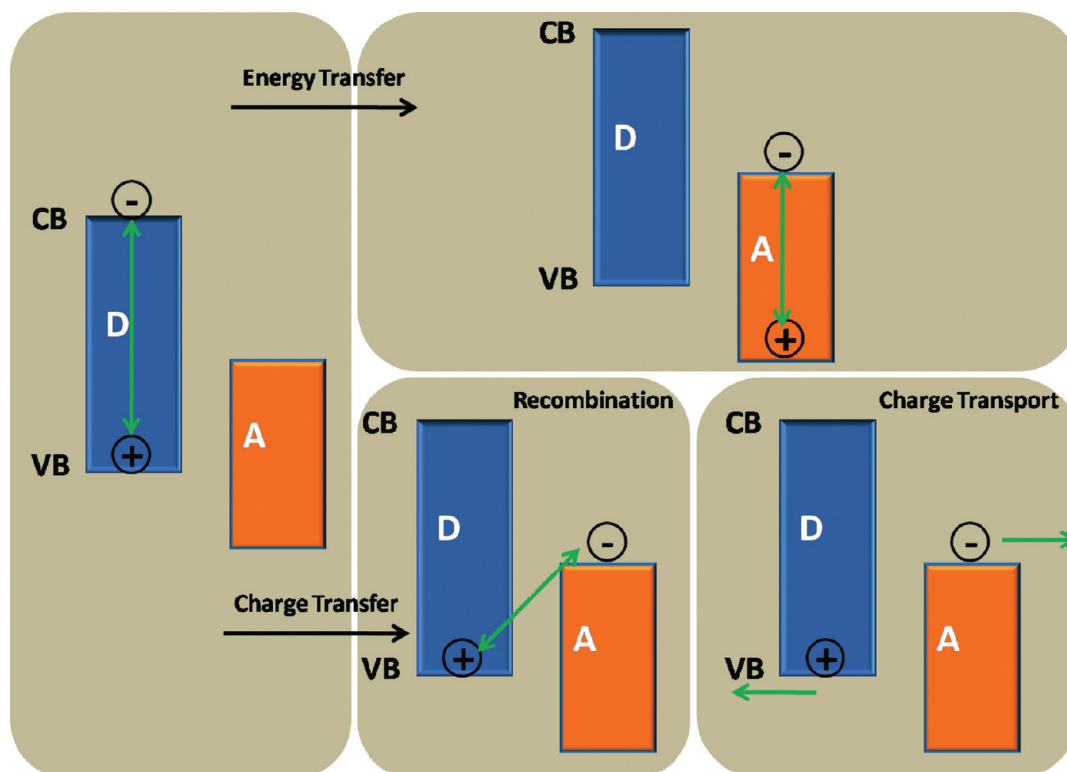


**Figure 15.** Schematic diagram of energy transfer and charge transfer of excitons. Energy transfer happens when excitons transferred from the donor to the acceptor for recombination, and charge transfer happens for recombination or dissociation of electrons and holes moving in the opposite direction.

holes settle on the valence band and the conduction band of the donor recombine and move to the valence band and the conduction band of the acceptor (see Figure 15). Transferred electrons and holes from the donor to the acceptor recombine radiatively or nonradiatively in a short time on the acceptor material.

Unlike type 1 (where the valence band of the donor is set lower than that of the acceptor, and the conduction band of the donor is set higher than that of the acceptor), photogenerated excitons of the donor do not move to the acceptor when both the valence band and the conduction band of the acceptor are set to a lower position than those of the donor. When the band offset energy is greater than the exciton binding energy, photogenerated electrons could be transferred from the conduction band of the donor to that of the acceptor. However, photogenerated holes are transferred from the valence band of the acceptor to the donor, instead of being transferred from the donor to the acceptor. Transferred electrons can be recombined with the holes remain in the valence band of the donor or dissociated electrons and holes are collected in each other ends. Such separated electrons and holes flow opposite to each other, and it is available for photovoltaic application.

**3.1. Charge Transfer in Nanoparticle Blends.** Alivisatos et al. first introduced a hybrid solar cell device using a blend of CdSe nanorods and polythiophene.<sup>107</sup> They mixed CdSe nanorods and poly(3-hexylthiophene) (P3HT) in a large interacting area of a charge transfer junction. The CdSe nanorod played the role of an electron acceptor and a hole donor, and P3HT acted as an electron donor and a hole acceptor. Solar cells were prepared by spin-coating 90 wt % of CdSe NCs in the solution of P3HT with poly(ethylene dioxythiophene):polystyrene sulfonic acid.

This solar cell showed over 54% external quantum efficiency and 6.9% power conversion efficiency at 515-nm illumination under 0.1 mW/cm<sup>2</sup>. It has also been reported that thiophene oligomers or dendrons are good combinations in improving charge-transfer properties in a hybrid NC system. A blend of CdSe NCs and polyfluorene copolymer also had a charge-transfer property.<sup>215</sup> A poly(2,7-(9,9-dioctyl-fluorene)-*alt*-5,5-(4',7'-di-2-thienyl-2',1',3'-benzothiadiazole)) and CdSe NC blend in chloroform was spin-coated on quartz glass. PL quenching of the polyfluorene copolymer was observed in this sample. Ninety percent (90%) of the polyfluorene copolymer's PL was quenched when the sample was prepared with 86 wt % of the NCs, because of the dissociation of the photogenerated excitons before they recombined. Hybrid photovoltaic device properties were examined by current density–voltage characteristics. The prepared film converted the incident photon to collect electrons with 40% efficiency in a broader spectral range of 510–590 nm and with a maximal value of 44% at 565 nm. This system also produced 2.4% power conversion efficiency. Poly(propylene vinylene) (PPV) is also a good source for charge transfer in a hybrid NC blend. Petrella et al. investigated charge transfer in a blend of CdS NCs and MEH-PPV.<sup>216</sup> Both the solution and the film state of the MEH-PPV/CdS NC blend showed significant fluorescence quenching of MEH-PPV, which can be explained by the charge transfer from polymer to NCs.

**3.2. Charge Transfer in Nanoparticles: Ligands and Cores.** Since the Alivisatos group first reported solar cell device preparation with CdSe nanorod and polythiophenes (see Figure 16a), there has been greater effort to optimize and improve the solar cell device performance, based on this proposed combination. One of the developing topics within this category is reducing the

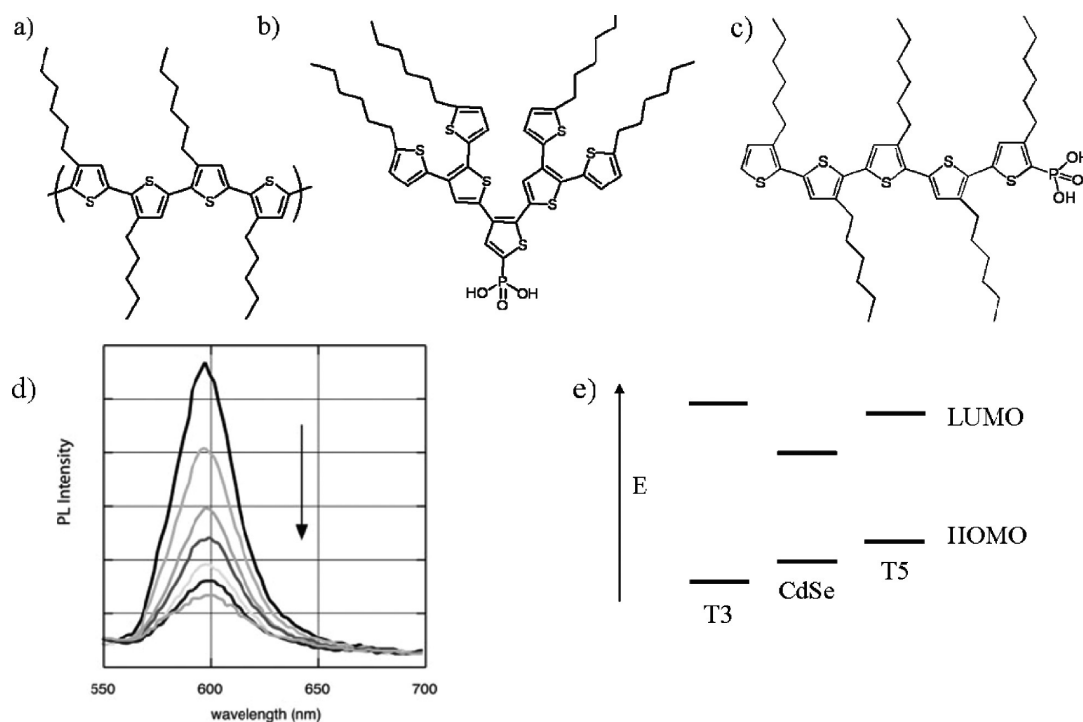


**Figure 16.** (a–c) Charge transfer in hybrid NCs with (a) polythiophene, (b) heptathiophene dendrons, and (c) pentathiophene. (d) Emission of CdSe NCs was quenched in CdSe-T5 hybrid. (e) HOMO–LUMO diagram of T3, T5, and CdSe NCs. Panels d and e have been adapted from ref 181, with permission from Wiley–VCH.

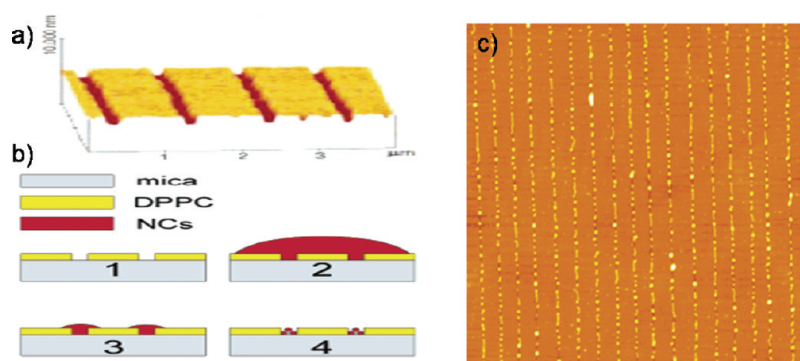


**Figure 17.** (a) SFM image of the channels between DPPC stripes. (b) Schematic figures of NPs patterning onto the prepatterned film. (c) SPM image of CdSe NC patterned film. (All panels have been adapted from ref 217, with permission from the American Chemical Society.)

size and the number of repeating units of thiophene oligomers and thiophene dendrons. Advincula et al. prepared CdSe NCs coated with nonlinear, cone-shaped thiophene dendrons, which have charge-transfer properties through ligand exchange.<sup>148</sup> They used second-generation thiophene dendrons for capping ligands, which have seven units of thiophene. Second-generation thiophene dendron, 2,3-di(*S,S'*-dihexyl-[2,2';3',2'']terthiophene-5'-yl)thiophenylphosphonic acid (P7T) (Figure 16b), replaced the TOPO from CdSe NCs. The prepared CdSe NCs are  $\sim 3.2$  nm in diameter and were capped with  $\sim 30$  units of P7T by ligand exchange. It was observed that the fluorescence from P7T and CdSe NCs was completely quenched by ligand-exchanged CdSe NCs. Again, this fluorescence quenching is due to the charge transfer between P7T ligands and CdSe NCs. Monolayered CdSe-P7T NC films were fabricated on an ITO substrate via spin coating to collect

current–voltage curves. This film showed an initial power conversion efficiency of 0.29%.

The number of thiophene units in the oligomer was even decreased to five by Alivisatos and Fréchet et al.<sup>181</sup> They prepared thiophene oligomers functionalized with hexyl groups for better solubility and phosphonic acid for capping CdSe NCs. Such prepared pentathiophene (T5) and terthiophene (T3) oligomers were shown to obtain a limiting number of thiophene units on thiophene oligomer, which allows for the charge-transfer property in CdSe NCs/thiophene oligomer hybrids (see Figure 16c). T3 and T5 functionalized with phosphonic acid replaced the TOPO from CdSe NCs by the LE method. The PL from thiophene oligomers was decreased in both hybrid NCs of CdSe-T3 and CdSe-T5. However, the fluorescence of CdSe increased when capped with T3, although the fluorescence of the

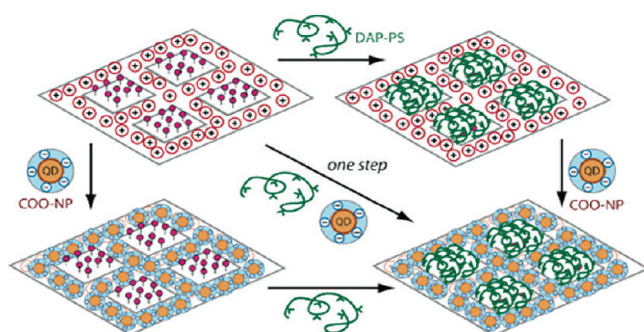


**Figure 18.** Schematic outline of patterned NC films by charging prepatterned substrates and nanoparticles. Adapted from ref 218, with permission from the American Chemical Society.

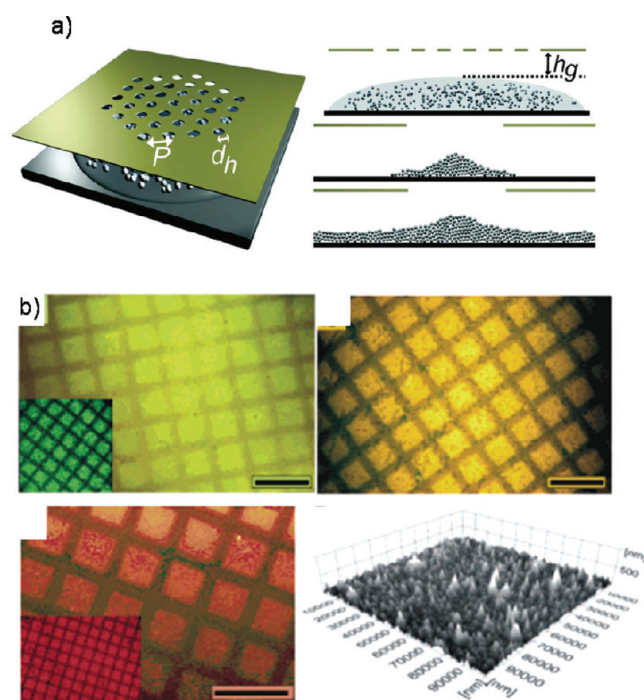


**Figure 19.** (a) Schematic outline of evaporative lithography process, and (b) fluorescence images of the patterned NC films by photolithography. (Panel a has been adapted from ref 219, with permission from the American Physical Society; panel b has been adapted from ref 220, with permission from the American Chemical Society.)

CdSe NCs was decreased when CdSe NCs were capped with T5 (see Figure 16d). These phenomena could be explained by an energy transfer mechanism in CdSe-T3 NCs and by a charge transfer process in CdSe-T5 NCs. It was explained that T3 has a lower HOMO level and T5 has a higher HOMO level, compared to the HOMO level of the CdSe NCs, since both T3 and T5 have a higher LUMO level than that of the CdSe NCs (see Figure 16e).

Ligand extension or ligand cross-linking on the surface of the NC tunes the optoelectronic properties of the NCs. Because optoelectronic properties are tunable with the number of thiophene units in the blend of thiophene oligomers and NCs, grafting thiophene oligomers from the NCs can shift the ET mechanism of NCs to charge transfer. Xu et al. grafted vinyl-terminated P3HT

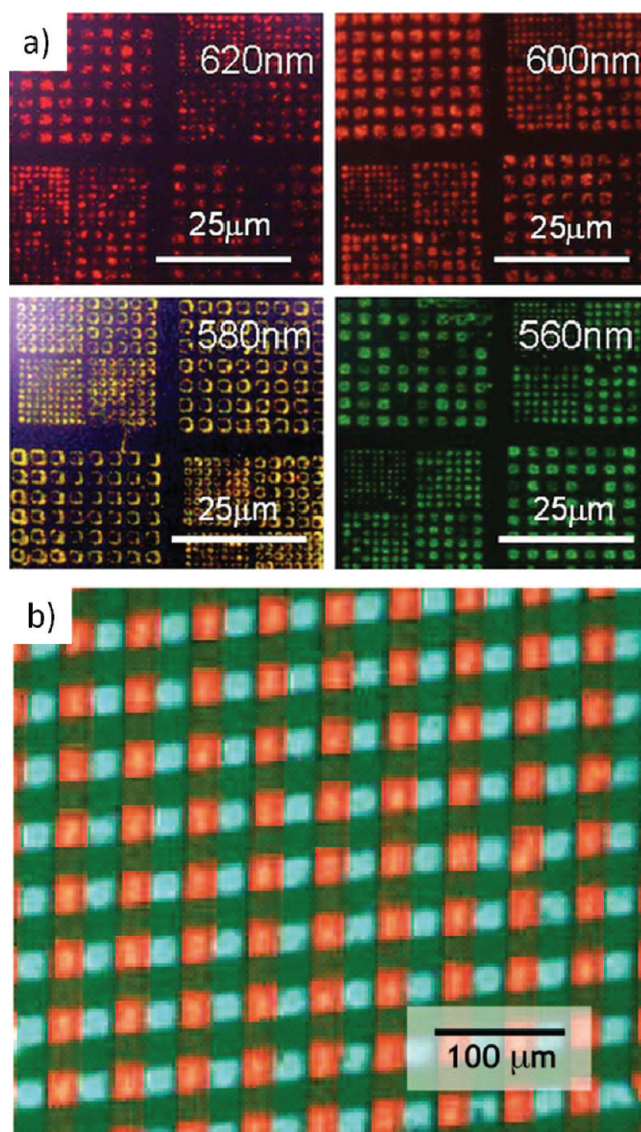


**Figure 20.** Electroluminescence of (a) nanopatterned LED with CdSe: ZnS core shell, (b) micropatterned with QDs on TPD. (Panel a has been adapted from ref 221, with permission from the American Institute of Physics; panel b has been adapted from ref 222, with permission from the American Chemical Society.)

from [(4-bromophenyl) methyl]dioctylphosphine oxide-capped CdSe NCs through Heck coupling in the presence of Pd catalyst.<sup>156</sup> They compared the optoelectronic properties of the P3HT-grafted CdSe NCs against the blend of P3HT and CdSe NCs. The blend of P3HT and CdSe NCs emitted light at a maximum at 670 nm and showed complete suppression of emission of the CdSe NCs due to energy transfer. However, two peaks, which are attributed to P3HT and CdSe NCs appeared in the case of the P3HT-grafted CdSe NCs. This was explained by a charge-transfer mechanism. Physical contact of P3HT to CdSe NCs allowed for induced electrons in excited P3HT to be directly injected onto the surface of CdSe NCs to passivate traps. Such passivation of the surface of the NCs increased the emission of CdSe NCs as in the case of P3HT-grafted CdSe NCs. They compared time-resolved PL lifetime of pristine P3HT, P3HT-grafted CdSe (CdSe-P3HT) NCs, and the



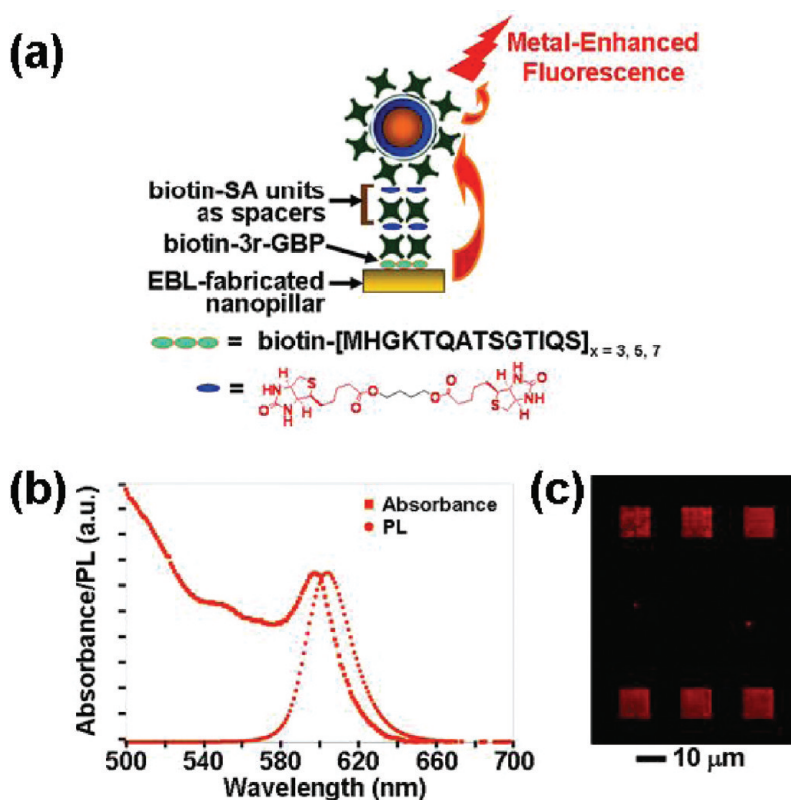


**Figure 21.** Biomolecular recognition of QDs on the patterned substrate: (a) scheme of SA functionalized QD assembly, (b) spectra of QDs, and (c) fluorescence image of QD arrays. (All panels have been adapted from ref 226, with permission from SPIE.)

blend of P3HT and CdSe NCs (CdSe/P3HT), and the average lifetimes of P3HT, CdSe-P3HT, and CdSe/P3HT were 240, 160, and 490 ps, respectively. The charge transfer efficiency of CdSe-P3HT was increased by  $\sim 33.3\%$ , based on the time-resolved PL lifetime data, compared to the pristine polymer. However, the lifetime of CdSe/P3HT blend was longer than that of pristine polymer, which indicates hindered charge transfer between NCs and polymers due to the ligands. Cross-linked organic ligands on the surface of the NCs also shifted the optoelectronic properties of the NCs. The ET mechanism of carbazole-bearing second-generation Fréchet-type dendron-capped CdSe NCs could be tuned by charge transfer of CdSe NCs through electropolymerization of the peripheral carbazole subunits on the surface of the CdSe NCs.<sup>148</sup> Because of the energy transfer from the dendron to the CdSe NCs, the emission of CdSe NCs increased, although the emission of the carbazole subunits decreased with increasing concentration of the NCs. However, the emission of the CdSe NCs also decreased after electropolymerization due to the charge transfer. The HOMO of the carbazole was shifted to a higher level than that of CdSe NCs by electrochemistry (electropolymerization to form polycarbazole), since nonelectrochemically treated carbazole had a lower HOMO level than that of the CdSe NCs.

#### 4. PATTERNING OF HYBRID NANOPARTICLE FILMS

It is important to demonstrate patterning of a thin film with hybrid materials for device applications. Prepatterned substrates have been used to build patterned hybrid NP films. Chi et al. adopted a nonlithographic approach to deposit CdSe NCs or CdSe/ZnS core-shell NCs on selective regions.<sup>217</sup> 1- $\alpha$ -Dipalmitoyl-phosphatidylcholine (DPPC) films were

fabricated using mica substrates, and the LB technique was used as the prepatterned substrate. The dilute NC solution was drop-cast onto the prepatterned film on the mica substrates. They succeeded in depositing NCs on selective positions of channels 150–200 nm wide in heights of 2 nm (see Figure 17).

It was also possible to achieve a stronger interaction between NCs and patterned substrates by ionizing the substrates and NCs. Rotello et al. used the positively charged, prepatterned substrates and the negatively charged NCs to form a more stable NC patterned film.<sup>218</sup> They patterned silica substrates with thymine and positively ionized N-methylpyridinium (PVMP) through photolithography. The PVMP remaining area was positively charged, as shown in Figure 18, and the carboxylate-derivatized CdSe/ZnS core-shell NCs were deposited onto the prepatterned film. Applying the negatively charged NCs to the positively charged substrates allowed electrostatic interaction between the NCs and substrates on selective patterns with 25- $\mu\text{m}$ -wide features.

Since the methods require the preparation of prepatterned films, several lithographical methods have also been introduced. Lewis et al. reported an evaporative lithography method for patterned NC film preparation.<sup>219</sup> They prepared NC patterned films by evaporative lithography through a mask. The holes in the mask had a diameter of 250  $\mu\text{m}$ . The pattern size could be also controlled by applying NCs solution in different concentrations. Using less-concentrated NCs, they could achieve smaller-sized NC patterns (see Figure 19). Kotov et al. suggested the method of photolithography for NC film patterning.<sup>220</sup> They prepared LBL films with CdSe/CdS NCs and PDDA on the glass slide. A

table lamp light (60 W) was irradiated for 72 h onto the NC film through a mask. They could tune the emitting color of the patterned film by controlling the irradiation time (see Figure 19).

Besides the referred methods, a stamping technique has been adopted to prepare a patterned QD NC structure for LED devices.<sup>221–224</sup> Gopal et al. deposited CdSe:ZnS core–shell colloidal QDs on the SiO<sub>2</sub> via microcontact printing (see Figure 20a). They could obtain electroluminescence from nano-patterned LED samples. Turn-on voltages were 3–4.5 V with NC average diameters of 7.8–9.8 nm.<sup>221</sup> Kim et al. also prepared micropatterned LED device via a contact printing method.<sup>222</sup> They printed CdSe/ZnS core–shell (red) and ZnSe/CdSe/ZnS core–double shell (green) onto the N,N'-bis(3-methylphenyl)-N,N'-bis(phenyl)benzidine (TPD)(blue) film in 25  $\mu$ m width. They observed the electroluminescence of red and green from quantum dot arrays and blue from TPD film when the LED was biased at 7 V (see Figure 20b).

As mentioned previously, energy transfer through bioligands or spacers in nanoparticles–nanoparticles or nanoparticles–metal system is applicable for biosensor.<sup>208,225</sup> Biosensor preparation with a 2D patterned film is possible, based on this chemistry. Jen and co-workers observed the fluorescence of streptavidin (SA) functionalized QDs assembled on the nanopatterned substrate via biotin–streptavidin interaction, as shown in Figure 21.<sup>226</sup> Biomolecular recognition allowed SA-functionalized QDs to emit fluorescence on the patterned structure.

The Advincula group has reported the preparation of conjugated polymer networks (CPNs) with linear<sup>227–233</sup> or dendritic polymers<sup>234–236</sup> via an electrochemical method. Since Alivisatos reported QD solar cells with polythiophene, Fréché and co-workers reported that the energy-transfer and charge-transfer mechanism of CdSe-oligothiophene can be shifted by controlling the number of thiophenes in the oligomer,<sup>181</sup> and our group reported similar optoelectronic property shift by increasing the number of carbazole units on the surface of QDs by electrochemistry.<sup>168</sup> Monomers on the surface of QDs and CPNs can be patterned on substrates by electrochemistry.<sup>227–233</sup> Therefore, electrochemistry would be one of the promising method for the preparation of the QD patterned device with controlling optoelectronic properties.

## 5. CONCLUSION

The efficient communication between semiconducting nanocomposites (NCs) and organic molecules in a hybrid material promotes a synergistic effect in their optoelectronic properties and application. The energy transfer (ET) between highly conjugated optically active organic polymers and semiconducting NCs creates a hybrid system with enhanced chemical and physical properties. The homogeneous dispersion of hybridized NCs in an organic polymer matrix facilitates better effective energy transfer. The application of organic dendrons as capping ligands to the NCs increases the surface area of the hybrid material and promotes energy transfer or charge transfer in the system effectively. Optoelectronically active organic ligands can be placed on the surfaces of NCs via a direct synthetic method or through either the “grafting to” or “grafting from” methods. More-complex organic ligands or polymers can replace the original capping ligands on the nanoparticles by ligand exchange. In another route, functional organic polymers were extended on the surfaces of NCs by polymerization. In addition, the chemical interaction allows ET among the NCs. The ET mechanism can

potentially be tuned by controlling the conduction band–valence band (CB–VB) or highest occupied molecular orbital–lowest unoccupied molecular orbital (HOMO–LUMO) band gap of the semiconducting NCs and organic molecules. Excitons, which are electron–hole pairs, can be transferred from the donor to the acceptor and can either recombine in the acceptor material or be separated from each other for electron isolation. Hybrid materials are also applicable to the preparation of films with specific optoelectronic properties. Furthermore, the two-dimensional patterning of these hybrid films makes further optoelectronic applications possible.

## AUTHOR INFORMATION

### Corresponding Author

\*Tel.: 713-743-1755. E-mail: radvincula@uh.edu.

## ACKNOWLEDGMENT

The authors gratefully acknowledge efforts by past group members and collaborators in hybrid nanoparticle synthesis and characterization. Research funding from the Robert A. Welch Foundation (E-1551), NSF-DMR-10-06776, CBET-0854979, and Texas NHARP 01846 is acknowledged. Technical support from KSV Instruments (Attension/Biolin Scientific), Agilent Technologies, Optrel GmbH, and Inficon, Inc. is also acknowledged.

## REFERENCES

- (1) Aleman, J.; Chadwick, A. V.; He, J.; Hess, M.; Horie, K.; Jones, R. G.; Kratochvil, P.; Meisel, I.; Mita, I.; Moad, G.; Penczek, S.; Stepto, R. F. T. *Pure Appl. Chem.* **2007**, *79* (10), 1801–1829.
- (2) Yu, G.; Gao, J.; Hummelen, J. C.; Wudl, F.; Heeger, A. J. *Science* **1995**, *270*, 1789–1791.
- (3) Hoppe, H.; Niggemann, M.; Winder, C.; Kraut, J.; Hiesgen, R.; Hinsch, A.; Meissner, D.; Sariciftci, N. S. *Adv. Funct. Mater.* **2004**, *14*, 1005–1011.
- (4) Yang, X. N.; van Duren, J. K. J.; Janssen, R. A. J.; Michels, M. A. J.; Loos, J. *Macromolecules* **2004**, *37*, 2151–2158.
- (5) Nelson, J. *Science* **2001**, *293*, 1059–1060.
- (6) Sheng, C.-X.; Tong, M.; Singh, S.; Vardeny, V. *Phys. Rev. B* **2007**, *75*, 085206/1–085206/7.
- (7) Zoombelt, A. P.; Fonrodona, M.; Wienk, M. M.; Sieval, A. B.; Hummelen, J. C.; Janssen, A. J. *Org. Lett.* **2009**, *11*, 903–906.
- (8) Admassie, S.; Inganäs, O.; Mammo, W.; Perzon, E.; Andersson, M. R. *Synth. Met.* **2006**, *156*, 614–623.
- (9) Pal, S.; Kesti, T.; Maiti, M.; Zhang, F.; Inganäs, O.; Hellström, S.; Andersson, M. R.; Oswald, F.; Langa, F.; Österman, T.; Pascher, T.; Yartsev, A.; Sundström, V. *J. Am. Chem. Soc.* **2010**, *132*, 12440–12451.
- (10) Coffey, D. C.; Ferguson, A. J.; Kopidakis, N.; Rumbles, G. *ACS Nano* **2010**, *4*, 5437–5445.
- (11) Clarke, T. M.; Durrant, J. R. *Chem. Rev.* **2010**, *110*, 6736–6767.
- (12) Günes, S.; Neugebauer, H.; Sariciftci, N. S. *Chem. Rev.* **2007**, *107*, 1324–1338.
- (13) Nagarjuna, G.; Yurt, S.; Jadhav, K. G.; Venkataraman, D. *Macromolecules* **2010**, *43*, 8045–8050.
- (14) Narizzano, R.; Erokhin, V.; Nicolini, C. *J. Phys. Chem. B* **2005**, *109*, 15798–15802.
- (15) Advincula, R.; Xia, C.; Taranekekar, P.; Onishi, K.; Deng, S.; Baba, A.; Knoll, W. *Mater. Res. Soc. Symp. Proc.* **2003**, *734*, B2.10/1–B2.10/6.
- (16) Inaoka, S.; Advincula, R. *Macromolecules* **2002**, *35*, 2426–2428.
- (17) Osaka, I.; Takimiya, K.; McCullough, D. *Adv. Mater.* **2010**, *22*, 4993–4997.
- (18) Al-Hashimi, M.; Labram, J. G.; Watkins, S.; Motevalli, M.; Anthopoulos, T. D.; Heeney, M. *Org. Lett.* **2010**, *12*, 5478–5481.

- (19) Nakao, K.; Nishimura, M.; Tamachi, T.; Kuwatani, Y.; Miyasaka, H.; Nishinaga, T.; Lyoda, M. *J. Am. Chem. Soc.* **2006**, *128*, 16740–16747.
- (20) Ma, W.; Iyer, P. K.; Gong, X.; Liu, B.; Moses, D.; Bazan, G. C.; Heeger, A. J. *Adv. Mater.* **2005**, *17*, 274–277.
- (21) Wakimoto, T.; Ochi, H.; Kawami, S.; Ohata, H.; Nagayama, K.; Murayama, R.; Okuda, Y.; Nakada, H.; Tohma, T.; Naito, T.; Abiko, H. *J. Soc. Info. Display* **1997**, *5*, 235–240.
- (22) Li, Z.; Yang, J.; Hou, J. G.; Zhu, Q. *Chem.—Eur. J.* **2004**, *10*, 1592–1596.
- (23) Graham, T. J. *Chem. Soc.* **1864**, *17*, 318–327.
- (24) Varadan, V. K.; Chen, L.; Xie, J. *Nanomedicine: Design and Applications of Magnetic Nanomaterials, Nanosensors, and Nanosystems*; John Wiley & Sons: New York, 2008; Chapter 1.
- (25) Fojtik, A.; Henglein, A. *Ber. Bunsen—Ges. Phys. Chem.* **1993**, *97*, 252–254.
- (26) Sibbald, M. S.; Chumanov, G.; Cotton, T. M. *J. Phys. Chem.* **1996**, *100*, 4672–4678.
- (27) Singh, S. C.; Swarnkar, R. K.; Gopal, R. *Bull. Mater. Sci.* **2010**, *33*, 21–26.
- (28) Kumar, P.; Huber, P. J. *Nanomater.* **2007**, 89718–1–89719–4.
- (29) Ould-Ely, T.; Thurston, J. H.; Kumar, A.; Respaud, M.; Guo, W. H.; Weidenthaler, C.; Whitmire, K. H. *Chem. Mater.* **2005**, *17*, 4750–4754.
- (30) Ru, Q. *Appl. Phys. Lett.* **1997**, *71*, 1792–1794.
- (31) Pan, Z. W.; Dai, Z. R.; Wang, Z. L. *Appl. Phys. Lett.* **2002**, *80*, 309–311.
- (32) Li, Y. D.; Wang, J. W.; Deng, Z. X.; Wu, Y. Y.; Sun, X. M.; Yu, D. P.; Yang, P. D. *J. Am. Chem. Soc.* **2001**, *123*, 9904–9905.
- (33) Piner, R. D.; Zhu, J.; Xu, F.; Hong, S.; Mirkin, C. A. *Science* **1999**, *283*, 661–663.
- (34) Ginger, D. S.; Zhang, H.; Mirkin, C. A. *Angew. Chem., Int. Ed.* **2004**, *43*, 30–45.
- (35) Vives, G.; Tour, J. M. *Acc. Chem. Res.* **2009**, *42*, 473–487.
- (36) Holder, E.; Tessler, N.; Rogach, A. L. *J. Mater. Chem.* **2008**, *18*, 1064–1078.
- (37) Advincula, R. *Dalton Trans.* **2006**, *23*, 2778–2784.
- (38) Yoshida, T.; Zhang, J.; Komatsu, D.; Sawatani, S.; Minoura, H.; Pauporté, T.; Lincot, D.; Oekermann, T.; Schlettwein, D.; Tada, H.; Wöhrle, D.; Funabiki, K.; Matsui, M.; Miura, H.; Yanagi, H. *Adv. Funct. Mater.* **2009**, *19*, 17–43.
- (39) Kongkanand, A.; Tvrdy, K.; Takechi, K.; Kuno, M.; Kamat, P. V. *J. Am. Chem. Soc.* **2008**, *130*, 4007–4015.
- (40) Schadler, L. S. *Nanocomposite Science and Technology*; Wiley—VCH; Weinheim, Germany, 2003; Chapter 2.
- (41) Crosby, A. J.; Lee, J. Y. *Polym. Rev.* **2007**, *47*, 217–229.
- (42) Larson, D. R.; Zipfel, W. R.; Williams, R. M.; Clark, S. W.; Bruchez, M. P.; Wise, F. W.; Webb, W. W. *Science* **2003**, *300*, 1434–1436.
- (43) Dayal, S.; Burda, C. J. *Am. Chem. Soc.* **2008**, *130*, 2890–2891.
- (44) Edwards, J. H.; Badwal, S. P. S.; Duffy, G. J.; Lasich, J.; Ganakas, G. *Solid State Ionics* **2002**, *152*–153, 843–852.
- (45) Dell, R. M.; Rand, D. A. J. *J. Power Sources* **2001**, *100*, 2–17.
- (46) Seddon, A. B. *IEEE Proc. Circuits Devices Syst.* **1998**, *145*, 369.
- (47) Andrews, M. P. *Proc. SPIE—Int. Soc. Opt. Eng. (U.S.A.)* **1997**, *2997*, 48–59.
- (48) Kang, K.; Kepner, A. D.; Hu, Y. Z.; Koch, S. W.; Peyghambarian, N.; Li, C.-Y.; Takada, T.; Kao, Y.; Mackenzie, J. D. *Appl. Phys. Lett.* **1994**, *64*, 1487–1489.
- (49) Butty, J.; Peyghambarian, N.; Kao, Y. H.; Mackenzie, J. D. *Appl. Phys. Lett.* **1996**, *69*, 3224–3226.
- (50) Wang, Y.; Herron, N. J. *Nonlinear Opt. Phys.* **1992**, *1*, 683–698.
- (51) Herron, N.; Thorn, D. L. *Adv. Mater.* **1998**, *10*, 1173–1184.
- (52) Colvin, V.; Schlamp, M.; Alivisatos, A. P. *Nature* **1994**, *370*, 354–378.
- (53) Dabbousi, B. O.; Bawendi, M. G.; Onitduka, O.; Rubner, M. F. *Appl. Phys. Lett.* **1996**, *66*, 1316–1318.
- (54) Coe, S.; Woo, W.-K.; Bawendi, M.; Bulović, V. *Nature* **2002**, *420*, 800–803.
- (55) Dai, Q.; Duty, C. E.; Hu, M. Z. *Small* **2010**, *6*, 1577–1588.
- (56) Carter, S. A.; Scott, J. C.; Brock, P. J. *Appl. Phys. Lett.* **1997**, *71*, 1145–1147.
- (57) Bliznyuk, V. B.; Ruhstaller, B.; Brock, P. J.; Scherf, U.; Carter, S. A. *Adv. Mater.* **1999**, *11*, 1257–1261.
- (58) Schlamp, M.; Peng, X.; Alivisatos, A. P. *J. Appl. Phys.* **1997**, *82*, S837–S842.
- (59) Mattoussi, H.; Radzilowski, L. H.; Dabbousi, B. O.; Fogg, D. E.; Schrock, R. R.; Thomas, E. L.; Bawendi, M. G.; Rubner, M. F. *J. Appl. Phys.* **1998**, *83*, 7965–7974.
- (60) Anikeeva, P. O.; Halpert, J. E.; Bawendi, M. G.; Bulović, V. *Nano Lett.* **2009**, *9*, 2532–2536.
- (61) Zou, H.; Wu, S.; Shen, J. *Chem. Rev.* **2008**, *108*, 3893–3957.
- (62) Motakef, S.; Boulton, J. M.; Uhlmann, D. R. *Opt. Lett.* **1994**, *19*, 1125–1127.
- (63) Roscher, C.; Buestrich, R.; Dannberg, P.; Rösch, O.; Popall, M. *Mater. Res. Soc. Symp. Proc.* **1998**, *519*, 239–244.
- (64) Asuka, K.; Liu, B. P.; Terano, M.; Nitta, K. H. *Macromol. Rapid Commun.* **2006**, *27*, 910–913.
- (65) Saito, R.; Kuwano, K.; Tobe, T. *J. Macromol. Sci. Pure Appl. Chem.* **2002**, *A39*, 171–182.
- (66) Shang, X. Y.; Zhu, Z. K.; Yin, J.; Ma, X. D. *Chem. Mater.* **2002**, *14*, 71–77.
- (67) Chang, C. C.; Chen, W. C. *Chem. Mater.* **2002**, *14*, 4242–4248.
- (68) Hochbaum, A. I.; Yang, P. *Chem. Rev.* **2010**, *110*, S27–S46.
- (69) Xia, Y.; Yang, P.; Sun, Y.; Wu, Y.; Mayers, B.; Gates, B.; Yin, Y.; Kim, F.; Yan, H. *Adv. Mater.* **2003**, *15*, 353–389.
- (70) Peña, O.; Pal, U.; Rodríguez-Fernández, L.; Crespo-Sosa, A. *J. Opt. Soc. Am. B* **2008**, *25*, 1371–1379.
- (71) Oldenburg, S. J.; Jackson, J. B.; Westcott, S. L.; Halas, N. J. *Appl. Phys. Lett.* **1999**, *75*, 2897–2899.
- (72) Oldenburg, S. J.; Averitt, R. D.; Westcott, S. L.; Halas, N. J. *Chem. Phys. Lett.* **1998**, *288*, 243–247.
- (73) Sun, Y.; Xia, Y. *Science* **2002**, *298*, 2176–2179.
- (74) El-Sayed, M. A. *Acc. Chem. Res.* **2001**, *34*, 257–264.
- (75) Ramachandra Rao, C. N.; Kulkarni, G. U.; Thomas, P. J.; Edwards, P. P. *Chem. Soc. Rev.* **2000**, *29*, 27–35.
- (76) Zhang, X.; Wang, P.; Zhang, X.; Xu, J.; Zhu, Y.; Yu, D. *Nano Res.* **2009**, *2*, 47–53.
- (77) Xu, Q.; Bao, J.; Capasso, F.; Whitesides, G. M. *Angew. Chem.* **2006**, *118*, 3713–3717.
- (78) Hu, Y.; Fleming, R. C.; Drezek, R. A. *Opt. Express* **2008**, *16*, 19579–19591.
- (79) Oldenburg, A. L.; Hansen, M. N.; Wei, A.; Boppert, S. A. *Proc. SPIE* **2007**, *6429*, 64291Z/1–64291Z/8.
- (80) Yu, E. T.; Derkacs, D.; Lim, S. H.; Matheu, P.; Schaadt, D. M. *Proc. SPIE* **2008**, *7033*, 70331V/1–70331V/9.
- (81) Yim, T.-J.; Wang, Y.; Zhang, X. *Nanotechnology* **2008**, *19*, 435605/1–435605/6.
- (82) McLellan, E.; Gunnarsson, L.; Rindzevicius, T.; Kall, M.; Zou, S.; Spears, K.; Schatz, G.; Van Duyne, R. *Mater. Res. Soc. Symp. Proc.* **2001**, *951*, 0951-E09–0951-E20.
- (83) Ghoshal, A.; Kik, P. G. *J. Appl. Phys.* **2008**, *103*, 113111/1–8.
- (84) Maier, S. A.; Kik, P. G.; Atwater, H. A. *Appl. Phys. Lett.* **2002**, *81*, 1714–1716.
- (85) Günes, S.; Sariciftci, N. S. *Inorg. Chim. Acta* **2008**, *361*, S81–S88.
- (86) Green, M. *Progr. Photovolt.* **2001**, *9*, 123–125.
- (87) Sariciftci, N. S.; Smilowitz, L.; Heeger, A. J.; Wudl, F. *Science* **1992**, *258*, 1474–1476.
- (88) Palaniappan, K.; Murphy, J. W.; Khanam, N.; Horvath, J.; Alshareef, H.; Quevedo-Lopez, M.; Biewer, M. C.; Park, S. Y.; Kim, M. J.; Gnade, B. E.; Stefan, M. C. *Macromolecules* **2009**, *42*, 3845–3848.
- (89) Clarke, T. M.; Durrant, J. R. *Chem. Rev.* **2010**, *110*, 6736–6767.
- (90) Parmer, J. E.; Mayer, A. C.; Hardin, B. E.; Scully, S. R.; McGehee, M. D.; Heeney, M.; McCulloch, I. *Appl. Phys. Lett.* **2008**, *92*, 113309/1–3.
- (91) Ma, W.; Yang, C.; Gong, X.; Lee, K.; Heeger, A. J. *Adv. Funct. Mater.* **2005**, *15*, 1665–1670.



- (92) Li, G.; Shrotriya, V.; Huang, J.; Yao, Y.; Moriart, T.; Emery, K.; Yang, Y. *Nat. Mater.* **2005**, *4*, 864–868.
- (93) Reyes-Reyes, M.; Kim, K.; Dewald, J.; López-Sandoval, R.; Avadhanula, A.; Curran, S.; Carrol, D. L. *Org. Lett.* **2005**, *7*, 5749–5752.
- (94) Kim, J. Y.; Kim, S. H.; Lee, H.-H.; Lee, K.; Ma, W.; Gong, X.; Hegger, A. J. *Adv. Mater.* **2006**, *18*, 572–576.
- (95) Peet, J.; Kim, J. Y.; Coates, N. E.; Ma, W. L.; Moses, D.; Heeger, A. J.; Bazan, G. C. *Nat. Mater.* **2007**, *6*, 497–500.
- (96) O'Regan, B.; Grätzel, M. *Nature* **1991**, *353*, 737–740.
- (97) Kamat, P. V. *J. Phys. Chem. C* **2008**, *112*, 18737–18753.
- (98) Gopidas, K. R.; Bohorquez, M.; Kamat, P. V. *J. Phys. Chem.* **1990**, *94*, 6435–6440.
- (99) Vinodgopal, K.; Kamat, P. V. *Environ. Sci. Technol.* **1995**, *29*, 841–845.
- (100) Bedja, I.; Kamat, P. V. *J. Phys. Chem.* **1995**, *99*, 9182–9188.
- (101) Vinodgopal, K.; Bedja, I.; Kamat, P. V. *Chem. Mater.* **1996**, *8*, 2180–2187.
- (102) Nasr, C.; Hotchandani, S.; Kim, W. Y.; Schmehl, R. H.; Kamat, P. V. *J. Phys. Chem. B* **1997**, *101*, 7480–7487.
- (103) Sant, P. A.; Kamat, P. V. *Phys. Chem. Chem. Phys.* **2002**, *4*, 198–203.
- (104) Gebeyehu, D.; Barbec, C.; Sariciftci, N. S.; Vangeneugden, D.; Kiebooms, R.; Vanderzande, D.; Kienberger, F.; Schindler, H. *Synth. Met.* **2002**, *125*, 279–287.
- (105) Beek, W. J. E.; Wienk, M. M.; Janssen, R. A. J. *Adv. Funct. Mater.* **2006**, *16*, 1112–1116.
- (106) Alivisatos, A. P. *Science* **1996**, *271*, 933–937.
- (107) Huynh, W.; Dittmer, J.; Alivisatos, A. P. *Science* **2002**, *295*, 2425–2427.
- (108) Greenham, N. C.; Peng, X.; Alivisatos, A. P. *Phys. Rev. B* **1996**, *54*, 17628–17637.
- (109) Smestad, G.; Spiekermann, S.; Kowalik, J.; Grant, C. D.; Schwartzberg, A. M.; Zhang, J.; Tolbert, L. M.; Moons, E. *Sol. Energy Mater. Sol. Cells* **2003**, *76*, 85–105.
- (110) Gebeyehu, D.; Barbec, C.; Sariciftci, N. S.; Vangeneugden, D.; Kiebooms, R.; Vanderzande, D.; Kienberger, F.; Schindler, H. *Synth. Met.* **2002**, *125*, 279–287.
- (111) Choi, J. J.; Lim, Y.-F.; Santiago-Berrios, M. B.; Oh, M.; Hyun, B.-R.; Sun, L.; Bartnik, A. C.; Goedhart, A.; Malliaras, G. G.; Abruña, A. D.; Wise, F. W.; Hanrath, T. *Nano Lett.* **2009**, *9*, 3749–3755.
- (112) Zhang, J.; Tang, C.; Bang, J. H. *Electrochem. Commun.* **2010**, *12*, 1124–1128.
- (113) Hwang, J.-Y.; Lee, S.-A.; Lee, Y. H.; Seok, S.-I. *ACS Appl. Mater. Interfaces* **2010**, *2*, 1343–1348.
- (114) Reda, S. M.; El-Sherbiny, S. A. *J. Mater. Res.* **2010**, *25*, 522–528.
- (115) Berney, C.; Danuser, G. *Biophys. J.* **2003**, *84*, 3992–4010.
- (116) Clapp, A.; Medintz, I.; Maru, J.; Fisher, B.; Bawendi, M.; Mattoussi, H. *J. Am. Chem. Soc.* **2004**, *126*, 301–310.
- (117) Lakowicz, J. *Principles of Fluorescence Spectroscopy*, 2nd ed.; Kluwer Academic Publishers: New York, 1999.
- (118) Saini, S.; Singh, H.; Bagchi, B. *J. Chem. Sci.* **2006**, *118*, 23–35.
- (119) Rose, A.; Tovar, J. D.; Yamaguchi, S.; Nesterov, E. E.; Zhu, Z.; Swager, T. M. *Philos. Trans. R. Soc. A* **2007**, *365*, 1589–1606.
- (120) Sicot, L.; Fiorini, C.; Lorin, A.; Nunzi, J. M.; Raimond, P.; Sentein, C. *Synth. Met.* **1999**, *102*, 991–992.
- (121) Choi, J.; Wang, N. S.; Reipa, V. *Langmuir* **2007**, *23*, 3388–3393.
- (122) Hao, E.; Schatz, G. C.; Hupp, J. T. *J. Fluoresc.* **2004**, *14*, 331–341.
- (123) Chen, X.; Mao, S. S. *Chem. Rev.* **2007**, *107*, 2891–2959.
- (124) Czerwosz, E.; Didusko, R.; Dłużewski, P.; Kęczkowska, J.; Rymarczyk, J.; Suchańska, M. *Vacuum* **2008**, *82*, 372–376.
- (125) Murray, C. B.; Sun, S.; Gaschler, W.; Doyle, H.; Betley, T. A.; Kagan, C. R. *IBM J. Res. Dev.* **2001**, *45*, 47–56.
- (126) Zhong, H.; Zhou, Y.; Ye, M.; He, Y.; Ye, J.; He, C.; Yang, C.; Li, Y. *Chem. Mater.* **2008**, *20*, 6434–6443.
- (127) Murray, C. B.; Norris, D. J.; Bawendi, M. G. *J. Am. Chem. Soc.* **1993**, *115*, 8706–8715.
- (128) Bruchez, M.; Moronne, M.; Gin, P.; Weiss, S.; Alivisatos, A. P. *Science* **1998**, *281*, 2013–2016.
- (129) Green, M.; O'Brien, P. J. *Chem. Soc., Chem. Commun.* **1999**, 2235–2241.
- (130) Hu, J.; Lu, Q.; Tang, K.; Qian, Y.; Zhou, G.; Liu, X. *J. Chem. Soc., Chem. Commun.* **1999**, 1093–1094.
- (131) Yang, J.; Cheng, G. H.; Zeng, J. H.; Yu, S. H.; Liu, X. M.; Qian, Y. T. *Chem. Mater.* **2001**, *13*, 848–853.
- (132) Faraday, M. *Philos. Trans. R. Soc. London* **1857**, *147*, 145–181.
- (133) Enustun, B. V.; Turkevich, J. *J. Am. Chem. Soc.* **1963**, *85*, 3317–3328.
- (134) Chen, J. P.; Lee, K. M.; Sorensen, C. M.; Klabunde, K. J.; Hadjipanayis, G. C. *J. Appl. Phys.* **1994**, *75*, 5876–5878.
- (135) Petit, C.; Taleb, A.; Pileni, M. P. *Adv. Mater.* **1998**, *10*, 259–261.
- (136) Sun, S.; Murray, C. B. *J. Appl. Phys.* **1999**, *85*, 4325–4330.
- (137) Pileni, M. P.; Ninham, B. W.; Gulik-Krzywicki, T.; Tanori, J.; Lisiecki, I.; Filankembo, A. *Adv. Mater.* **1999**, *11*, 1358–1362.
- (138) Khanna, P. K.; Singh, N.; Subbarao, V. V. S.; Gokhale, K.; Mulik, U. P. *Mater. Chem. Phys.* **2005**, *93*, 117–121.
- (139) Rogach, A. L. *Semiconductor Nanocrystal Quantum Dots Synthesis, Assembly, Spectroscopy and Applications*; Springer, and Wien: New York, 2008.
- (140) Bowen Katari, J. E.; Colvin, V. L.; Alivisatos, A. P. *J. Phys. Chem.* **1994**, *98*, 4109–4117.
- (141) Talapin, D. V.; Rogach, A. L.; Kornowski, A.; Haase, M.; Weller, H. *Nano Lett.* **2001**, *1*, 207–211.
- (142) Peng, Z. A.; Peng, X. *J. Am. Chem. Soc.* **2001**, *123*, 183–184.
- (143) Qu, L.; Peng, Z. A.; Peng, X. *Nano Lett.* **2001**, *1*, 333–337.
- (144) Biju, V.; Makita, Y.; Sonoda, A.; Yokoyama, H.; Baba, Y.; Ishikawa, M. *J. Phys. Chem. B* **2005**, *109*, 13899–13905.
- (145) Yu, W. W.; Falkner, J. C.; Shih, S. S.; Colvin, V. L. *Chem. Mater.* **2004**, *16*, 3318–3322.
- (146) Steckel, J. S.; Coe-Sullivan, S.; Bulović, V.; Bawendi, M. G. *Adv. Mater.* **2003**, *15*, 1862–1866.
- (147) Larsen, T. H.; Sigman, M.; Ghezelbash, A.; Doty, R. C.; Korgel, B. A. *J. Am. Chem. Soc.* **2003**, *125*, 5638–5639.
- (148) Locklin, J.; Patton, D.; Deng, S.; Baba, A.; Millan, M.; Advincula, R. C. *Chem. Mater.* **2004**, *16*, 5187–5193.
- (149) Esteves, C. C.; Bombalski, L.; Trindade, T.; Matyjaszewski, K.; Barros-Timmons, A. *Small* **2007**, *7*, 1230–1236.
- (150) Skaff, H.; Emrick, T. *Angew. Chem., Int. Ed.* **2004**, *43*, 5383–5386.
- (151) Esteves, A. C. C.; Hodge, P.; Trindade, T.; Barros-Timmons, A. M. V. *J. Polym. Sci., Part A: Polym. Chem.* **2009**, *47*, 5367–5377.
- (152) Carrot, G.; Rutot-Houzé, D.; Pottier, A.; Degée, P.; Hilborn, J.; Dubois, P. *Macromolecules* **2002**, *35*, 8400–8404.
- (153) Skaff, H.; Ilker, M. F.; Coughlin, E. B.; Emrick, T. *J. Am. Chem. Soc.* **2002**, *124*, 5729–5733.
- (154) Zhou, L.; Gao, C.; Xu, W. *J. Mater. Chem.* **2009**, *19*, 5655–5664.
- (155) Skaff, H.; Sill, K.; Emrick, T. *J. Am. Chem. Soc.* **2004**, *126*, 11322–11325.
- (156) Xu, J.; Wang, J.; Mitchell, M.; Mukherjee, P.; Jeffries-EL, M.; Petrich, J. W.; Lin, Z. *J. Am. Chem. Soc.* **2007**, *129*, 12828–12833.
- (157) Jun, W.-Y.; Choi, J.-S.; Cheon, J. *Angew. Chem., Int. Ed.* **2006**, *45*, 3414–3439.
- (158) Costi, R.; Saunders, A. E.; Banin, U. *Angew. Chem., Int. Ed.* **2010**, *49*, 4878–4897.
- (159) Ray, P. C. *Chem. Rev.* **2010**, *110*, 5332–5365.
- (160) Xiong, Y.; Wiley, B. J.; Xia, Y. *Angew. Chem., Int. Ed.* **2007**, *46*, 7157–7159.
- (161) Chestnoy, N.; Hull, R.; Brus, L. E. *J. Chem. Phys.* **1986**, *85*, 2237–2242.
- (162) Murray, C. B.; Norris, D. J.; Bawendi, M. G. *J. Am. Chem. Soc.* **1993**, *115*, 8706–8715.

- (163) Peng, X.; Manna, L.; Yang, W.; Wickham, J.; Scher, E.; Kadavanich, A.; Alivisatos, A. P. *Nature* **2000**, *404*, 59–61.
- (164) Peng, Z. A.; Peng, X. J. *Am. Chem. Soc.* **2002**, *124*, 3343–3353.
- (165) Liu, Z.; Boltasseva, A.; Pedersen, R. H.; Bakker, R.; Kildishev, A. V.; Drachev, V. P.; Shalae, V. M. *Metamaterials* **2008**, *2*, 45–51.
- (166) Manna, L.; Milliron, D. J.; Meisel, A.; Scher, E. C.; Alivisatos, A. P. *Nat. Mater.* **2003**, *2*, 382–385.
- (167) Asokan, S.; Krueger, K. M.; Colvin, V. L.; Wong, M. S. *Small* **2007**, *3*, 1164–1169.
- (168) Park, Y.; Taranekekar, P.; Park, J.; Baba, A.; Fulghum, T.; Advincula, R. C. *Adv. Funct. Mater.* **2008**, *18*, 2071–2078.
- (169) Park, J. H.; Park, O. O.; Kim, J. K.; Yu, J.-W.; Kim, J. Y.; Kim, Y. C. *J. Nonlinear Opt. Phys. Mater.* **2005**, *14*, 481–486.
- (170) Tang, A. W.; Teng, F.; Xiong, S.; Gao, Y. H.; Liang, C. J.; Hou, Y. B. *J. Photochem. Photobiol. A* **2007**, *192*, 1–7.
- (171) Teng, F.; Tang, A.; Feng, B.; Lou, Z. *Appl. Surf. Sci.* **2008**, *254*, 6341–6345.
- (172) McDonald, S. A.; Cyr, P. W.; Levina, L.; Sargent, E. H. *Appl. Phys. Lett.* **2004**, *85*, 2089–2091.
- (173) Bakueva, L.; Konstantatos, G.; Musikhin, S.; Ruda, H. E.; Shik, A. *Appl. Phys. Lett.* **2004**, *85*, 3567–3569.
- (174) Chang, F.; Musikhin, S.; Bakueva, L.; Levina, L.; Hines, M.; Cyr, P.; Sargent, E. *Appl. Phys. Lett.* **2004**, *84*, 4295–4297.
- (175) Warner, J. H.; Watt, A. R.; Thomsen, E.; Heckenberg, N.; Meredith, P.; Rubinsztajn-Dunlop, H. *J. Phys. Chem. B* **2005**, *109*, 9001–9005.
- (176) Anni, M.; Manna, L.; Cingolani, R.; Valerini, D.; Cretí, A.; Lomascolo, M. *Appl. Phys. Lett.* **2004**, *85*, 4169–4171.
- (177) Fang, C.; Zhao, B.-M.; Lu, H.-T.; Sai, L.-M.; Fan, Q.-L.; Wang, L.-H.; Huang, W. J. *Phys. Chem. C* **2008**, *112*, 7278–7283.
- (178) Fuke, N.; Hoch, L. B.; Kaposov, A. Y.; Manner, V. W.; Werder, D. J.; Fukui, A.; Koide, N.; Katayama, H.; Sykora, M. *ACS Nano* **2010**, *4*, 6377–6386.
- (179) Sudeep, P. K.; Emrick, T. *Polym. Rev.* **2007**, *47*, 155–163.
- (180) Hammer, N. I.; Emrick, T.; Barnes, M. D. *Nanoscale Res. Lett.* **2007**, *2*, 282–290.
- (181) Milliron, D. J.; Alivisatos, A. P.; Pitois, C.; Edder, C.; Fréchet, J. M. J. *Adv. Mater.* **2003**, *15*, 58–61.
- (182) Odoi, M. Y.; Hammer, N. I.; Sill, K.; Emrick, T.; Barnes, M. D. *J. Am. Chem. Soc.* **2006**, *128*, 3506–3507.
- (183) Li, J.; Liu, D. J. *Mater. Chem.* **2009**, *19*, 7584–7591.
- (184) Hecht, S.; Fréchet, J. M. J. *Angew. Chem., Int. Ed.* **2001**, *40*, 74–91.
- (185) Goodson, T. G. *Acc. Chem. Res.* **2005**, *38*, 99–107.
- (186) Katsuma, K.; Shirota, Y. *Adv. Mater.* **1998**, *10*, 223–226.
- (187) Zhang, Y.; Chen, Y.; Niu, H.; Gao, M. *Small* **2006**, *2*, 1314–1319.
- (188) Potapova, I.; Mruk, R.; Hübner, C.; Zentel, R.; Basché, T.; Mews, A. *Angew. Chem., Int. Ed.* **2005**, *44*, 2437–2440.
- (189) Funston, A. M.; Jasieniak, J. J.; Mulvaney, P. *Adv. Mater.* **2008**, *20*, 4274–4280.
- (190) Querner, C.; Reiss, P.; Zagorska, M.; Renault, O.; Payerne, R.; Genoud, F.; Rannou, P.; Pron, A. *J. Mater. Chem.* **2005**, *15*, 554–563.
- (191) Bachman, P. K.; Geittner, P.; Krafizynk, E.; Lydtin, H.; Romanowski, G. *Am. Ceram. Soc. Bull.* **1989**, *70*, 1826–1831.
- (192) Franzl, T.; Klar, T. A.; Schietinger, S.; Rogach, A. L.; Feldmann, J. *Nano Lett.* **2004**, *4*, 1599–1603.
- (193) Tang, B.; Cao, L.; Xu, K.; Zhou, L.; Ge, J.; Li, Q.; Yu, L. *Chem.—Eur. J.* **2008**, *14*, 3637–3644.
- (194) Park, J. H.; Park, S.-I.; Kim, T.-H.; Park, O. O. *Thin Solid Films* **2007**, *515*, 3085–3089.
- (195) Nikiforov, M. P.; Zerweck, U.; Milde, P.; Loppacher, C.; Park, T.-H.; Uyeda, H. T.; Therien, M. J.; Eng, L.; Bonnell, D. *Nano Lett.* **2008**, *8*, 110–113.
- (196) Juhl, A. T.; Busbee, J. D.; Koval, J. J.; Natarajan, L. V.; Tondiglia, V. P.; Vaia, R. A.; Bunning, T. J.; Braun, P. V. *ACS Nano* **2010**, *4*, 5953–5961.
- (197) Linn, N. C.; Sun, C.-H.; Arya, A.; Jiang, P.; Jiang, B. *Nanotechnology* **2009**, *20*, 255303–255306.
- (198) Banerjee, P.; Conklin, D.; Nanayakkara, S.; Park, T.-H.; Therien, M. J.; Bonnell, D. A. *ACS Nano* **2010**, *4*, 1019–1025.
- (199) Ghosh, S. K.; Pal, T. *Chem. Rev.* **2007**, *107*, 4797–4862.
- (200) Zabet-Khosousi, A.; Dhirani, A. A. *Chem. Rev.* **2008**, *108*, 4072–4124.
- (201) Rogach, A.; Klar, T. A.; Lupton, J. M.; Meijerink, A.; Feldmann, J. *J. Mater. Chem.* **2009**, *19*, 1208–1221.
- (202) Zhang, Q.; Atay, T.; Tischler, J. R.; Bradley, M. S.; Bulović, V.; Nurmikko, A. V. *Nature Nano.* **2007**, *2*, 555–559.
- (203) Dutton, P. J.; Conte, L. *Langmuir* **1999**, *15*, 613–617.
- (204) Zenker, R.; Sacher, G.; Buchwalder, A.; Liebich, J.; Reiter, A.; Hässler, R. *Surf. Coat. Technol.* **2007**, *202*, 804–808.
- (205) Crooker, S. A.; Hollingsworth, J. A.; Tretiak, S.; Klimov, V. I. *Phys. Rev. Lett.* **2002**, *89*, 186802/1–186802/4.
- (206) Gregg, B. A. *J. Phys. Chem. B* **2003**, *107*, 4688–4698.
- (207) Achermann, M.; Petruska, M. A.; Kos, S.; Smith, D. L.; Koleske, D. D.; Klimov, V. I. *Nature* **2004**, *429*, 642–646.
- (208) Gole, A.; Jana, N. R.; Selvan, S. T.; Ying, J. Y. *Langmuir* **2008**, *24*, 8181–8186.
- (209) Gledhill, S. E.; Scott, B.; Gregg, B. A. *J. Mater. Res.* **2005**, *20*, 3167–3179.
- (210) Gregg, B. A. *Mol. Comput. Electron. Devices* **2003**, *844*, 243.
- (211) Cahen, D.; Hodes, G.; Gratzel, M.; Guillemoles, J. F.; Reiss, I. *J. Phys. Chem. B* **2000**, *104*, 2053–2059.
- (212) Gregg, B. A.; Hanna, M. C. *J. Appl. Phys.* **2003**, *93*, 3605–3614.
- (213) Peumans, P.; Yakimov, A.; Forrest, S. R. *J. Appl. Phys.* **2003**, *93*, 3693–3723.
- (214) Kannan, B.; Castelimo, K.; Majumdar, A. *Nano Lett.* **2003**, *3*, 1729–1733.
- (215) Wang, P.; Abrusci, A.; Wong, H. M. P.; Svensson, M.; Andersson, M. R.; Greenham, N. C. *Nano Lett.* **2006**, *6*, 1789–1793.
- (216) Petrella, A.; Tamborra, M.; Cosma, P.; Curri, M. L.; Striccoli, M.; Comparelli, R.; Agostiano, A. *Thin Solid Films* **2008**, *516*, 5010–5015.
- (217) Lu, N.; Chen, X.; Molenda, D.; Naber, A.; Fuchs, H.; Talapin, D. V.; Weller, H.; Müller, J.; Lupton, J. M.; Feldmann, J.; Rogach, A. L.; Chi, L. *Nano Lett.* **2004**, *4*, 885–888.
- (218) Xu, H.; Hong, R.; Lu, T.; Uzun, O.; Rotello, V. M. *J. Am. Chem. Soc.* **2006**, *128*, 3162–3163.
- (219) Harris, D. J.; Hu, H.; Conrad, J. C.; Lewis, J. A. *Phys. Rev. Lett.* **2007**, *98*, 148301/1–148301/4.
- (220) Wang, Y.; Tang, Z.; Correa-Duarte, M. A.; Liz-Marzán, L. M.; Kotov, N. A. *J. Am. Chem. Soc.* **2003**, *125*, 2830–2831.
- (221) Gopal, A.; Hoshino, K.; Zhang, X. *Appl. Phys. Lett.* **2010**, *96*, 131109/1–3.
- (222) Kim, L.; Anikeeva, P. O.; Coe-Sullivan, S. A.; Steckel, J. S.; Bawendi, M. G.; Bulović, V. *Nano Lett.* **2008**, *8*, 4513–4517.
- (223) Gopal, A.; Hoshino, K.; Kim, S.; Zhang, X. *Nanotechnology* **2009**, *20*, 235201/1–235201/9.
- (224) Wood, V.; Panzer, M. J.; Chen, J.; Bradley, M. S.; Halpert, J. E.; Bawendi, M. G.; Bulović, V. *Adv. Mater.* **2009**, *21*, 2151–2155.
- (225) Oh, E.; Hong, M.-Y.; Lee, D.; Nam, S.-H.; Yoon, H. C.; Kim, H.-S. *J. Am. Chem. Soc.* **2005**, *127*, 3270–3271.
- (226) Leong, K.; Zin, M. T.; Ma, H.; Huang, F.; Sarikaya, M.; Jen, A. K.-Y. *Proc. SPIE* **2008**, *7040*, 704007/1–704007/12.
- (227) Huang, C.; Jiang, G.; Advincula, R. *Macromolecules* **2008**, *41*, 4661–4670.
- (228) Taranekekar, P.; Baba, A.; Fulghum, T. M.; Advincula, R. *Macromolecules* **2005**, *38*, 3679–3687.
- (229) Xia, C.; Advincula, R. C. *Chem. Mater.* **2001**, *13*, 1682–1691.
- (230) Deng, S.; Advincula, R. C. *Chem. Mater.* **2002**, *14*, 4073–4080.
- (231) Fulghum, T.; Karim, S. M. A.; Baba, A.; Taranekekar, P.; Nakai, T.; Masuda, T.; Advincula, R. C. *Macromolecules* **2006**, *39*, 1467–1473.
- (232) Inaoka, S.; Roitman, D. B.; Advincula, R. C. *Chem. Mater.* **2005**, *17*, 6781–6789.

- (233) Fulghum, T. M.; Taraneekar, P.; Advincula, R. C. *Macromolecules* **2008**, *41*, 5681–5687.
- (234) Taraneekar, P.; Park, J.-Y.; Patton, D.; Fulghum, T.; Ramon, G. J.; Advincula, R. *Adv. Mater.* **2006**, *18*, 2461–2465.
- (235) Taraneekar, P.; Baba, A.; Park, J. Y.; Fulghum, T.; Advincula, R. *Adv. Funct. Mater.* **2006**, *16*, 2000–2007.
- (236) Taraneekar, P.; Fulghum, T.; Patton, D.; Ponnampati, R.; Clyde, G.; Advincula, R. *J. Am. Chem. Soc.* **2007**, *129*, 12537–12548.